CHAPTER 3

SYNTHESIS AND REACTIVITY OF METAL COMPLEXES SUPPORTED BY A NON-INNOCENT HYDROQUINONE PARA-TERPHENYL DIPHOSPHINE LIGAND

Abstract

A novel *para*-terphenyl diphosphine ligand was synthesized with a non-innocent hydroquinone moiety as the central arene (**1-H**). *Pseudo*-tetrahedral 4-coordinate Ni^0 and Pd^0-quinone (**2** and **3**, respectively) complexes proved accessible by metalating **1-H** with the corresponding $M^{II}(OAc)_2$ precursors. O_2 does not react with the Pd^0-quinone species (**3**) and protonation occurs at the quinone moiety indicating that the coordinated oxidized quinonoid moiety prevents reactivity at the metal. A 2-coordinate Pd^0-hydroquinone complex (**4-H**) was prepared using a one-pot metalation with Pd^{II} followed by reduction. The reduced quinonoid moiety in **4-H** shows metal-coupled reactivity with small molecules. **4-H** was capable of reducing a variety of substrates including dioxygen, nitric oxide, nitrous oxide, 1-azido adamantane, trimethylamine *n*-oxide, and 1,4-benzoquinone quantitatively producing **3** as the Pd-containing reaction product. Mechanistic investigations of dioxygen reduction revealed that the reaction proceeds through a η^2-peroxo intermediate (**Int1**) at low temperatures followed by subsequent ligand oxidation at higher temperatures in a reaction that consumed half an equivalent of O_2 and produced water as a final oxygenic byproduct. Control compounds with methyl protected phenolic moieties (**4-Me**), displaying a Ag^I center incapable of O_2 binding (**7-H**) or a cationic Pd-H motif (**6-H**) allowed for the independent examination of potential reaction pathways. The reaction of **4-Me** with dioxygen at low temperature produces a species (**8-Me**) analogous to **Int1** demonstrating that initial dioxygen activation is an inner sphere Pd-based process where the hydroquinone moiety only subsequently participates in the reduction of O_2, at higher temperatures, by H^+/e^- transfers.

INTRODUCTION

Dioxygen is commonly employed as an oxidant in biology where active site architecture regulates the delivery of reducing equivalents and protons to the substrate.[1] Similar strategies for electron[2] or proton management[3] using non-innocent ligand frameworks have been developed in synthetic systems. However, ligands capable of both proton and electron transfers during small molecule activation remain uncommon.[3b, 4] Aerobic oxidation chemistry using Pd[5] has seen many advances recently due to the appeal of employing dioxygen as a stoichiometric oxidant in a strategy akin to biological oxidase catalysts. Pd-catalyzed aerobic oxidations utilizing the reversible two proton-two electron couple of 1,4-benzoquinone as an additive has important applications in organic methodology.[6] The use 1,4-benzoquinone and its derivatives as stoichiometric or catalytic oxidants in their own right has also recently been reviewed.[7] Recent mechanistic studies have highlighted the complicated reaction pathways available in the combination of redox active metal (Pd), redox active organic additive that can also act as ligand (1,4-benzoquinone), and O_2.[6a, 8] Although in catalysis with Pd, 1,4-benzoquinone is used as a direct oxidant, we are particularly interested in the reactivity of the reduced counterpart, as a venue for providing protons and electrons for substrate activation in the presence of a reactive metal site. At the same time, the effect of the nature of the quinonoid fragment (reduced vs oxidized) on the chemistry of Pd with O_2 is particularly relevant to organic methodology. To that end, proximity to the reactive metal site is instrumental. Efforts to directly incorporate quinonoid moieties into ligand frameworks for Pd have been reported.[9] Though the interconversion of the hydroquinone and quinone forms of these ligands has been observed in some instances, the reduction of dioxygen with these Pd systems has not been reported. The use of π-bound quinonoid moieties as ligands has seen a several applications.[10]

Our group has reported the use of bis- and trisphosphinoarylbenzene ligands as scaffolds for mono- and multinuclear, π-bound transition metal complexes.[11] Non-innocence of the central arene moiety has been observed with cationic Ni–H complexes with respect to H-migration as well as with dinuclear Fe and Co carbonyl complexes with respect to partial reduction of the ring.[11e, 11g] The incorporation of a catechol moiety into the ligand scaffold capable of transferring multiple electrons and protons or other electrophiles during dioxygen reduction has also been recently reported for a Mo complex.[11c] In that case, there is no evidence that the metal center undergoes inner sphere chemistry with O_2, although electronic coupling with the quinonoid moiety and transfer of electrophile from catechol is instrumental for reactivity. With its established inner sphere chemistry with O_2, Pd provides an ideal case study for the effect of a pendant non-innocent group capable of transferring both electrons and protons. Moreover, given the utilization of Pd, hydroquinone, and O_2 in catalysis the present studies have implications to organic methodology. We report the synthesis of a *para*-terphenyldiphosphine ligand containing a 1,4-hydroquinone moiety and the cooperative small molecule activation observed in a Pd^0 complex.

RESULTS AND DISCUSSION

Section 3.1 Ligand Synthesis

The desired ligand, **1-H** (Scheme 1), was readily synthesized in five steps from commercially available starting materials. 2,5-diiodo-1,4-hydroquinone was synthesized according to literature procedures in two steps from 1,4-dimethoxybenzene. Methoxymethyl acetal (MOM) protection of both OH moieties to produce compound **A** was accomplished in dichloromethane (DCM) using diisopropyl ethyl amine as the base. A palladium-catalyzed Suzuki coupling with 2-bromophenyl boronic acid as the coupling partner yielded the desired

terphenyl ligand precursor (**B**). Subsequent lithium halogen exchange with *tert*-butyl lithium (*t*BuLi) followed by addition the chloro diisopropyl phosphine yielded the desired ligand (**1-H**). Much like the dimethoxy variant presented in Chapter 2 (Section 2.1 **1-(OMe)$_2$**), hindered rotation results in multiple $^{31}P\{^1H\}$ resonances (1.80, -0.06 ppm) at room temperature as well as a broadened ^1H spectrum.

Scheme 1. Synthesis of 1-H

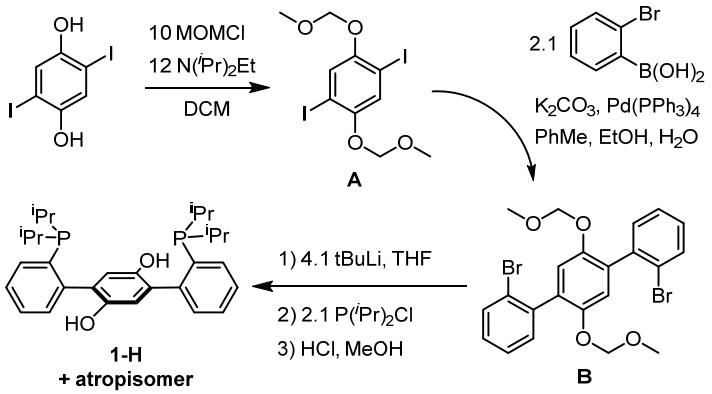

Section 3.2 Synthesis of Hydroquinone and Quinone Diphosphine-Supported Metal Complexes

Ni and Pd complexes supported by both the hydroquinone and quinone forms of compound **1-H** were targeted. Metalations with Ni^{II} or Pd^{II} diacetate proceeded in tetrahydrofuran (THF), though elevated temperatures were required for nickel. Both reactions yielded the corresponding M^0-quinone complexes **2** and **3** (~60% yield) as green and purple solids, respectively (Scheme 2).

The quinone assignment for the central arene was corroborated by strong ν_{CO} infrared (IR) absorptions at 1597 and 1603 cm^{-1} for complex **2** and **3** respectively. While the quinone form of **1-H** could not be isolated, likely due to reactivity with the phosphine moieties, a shift to lower ν_{CO} stretching frequencies relative to 2,5-diphenyl-1,4-benzoquinone (1640 cm^{-1})[12] is consistent with data reported for other π-bound Ni and Pd quinone complexes.[13] Solution

NMR data in CD_2Cl_2 for **2** and **3** are consistent with either C_2 symmetric structures or a fast exchange process on the NMR time scale that exchanges the front and back of the molecules (as drawn). Both complexes show sharp singlets (**2**: 6.13 ppm, **3**: 6.10 ppm) corresponding to the central quinone protons and two distinct methine resonances (**2**: 2.52, 2.24 ppm, **3**: 2.46, 2.33 ppm) in the ^1H NMR spectra. By $^{31}P\{^1H\}$ NMR, single resonances are observed at 54.30 and 55.02 ppm for **2** and **3** respectively. Strong metal-to-ligand charge transfer bands for both complexes give both complexes their distinct colors (**2**: ε_{389} = 5000 M^{-1} cm^{-1}, ε_{456} = 1700 M^{-1} cm^{-1}, ε_{623} = 650 M^{-1} cm^{-1}; **3**: ε_{316} = 8300 M^{-1} cm^{-1}, ε_{375} = 6200 M^{-1} cm^{-1}, ε_{544} = 2400 M^{-1} cm^{-1}).[14] Formally these metalations result in the two proton / two electron oxidation of the hydroquinone moiety with the acetates and the M^{II} center serving as the proton and electron acceptors respectively.

Scheme 2. Synthesis of reported metal complexes

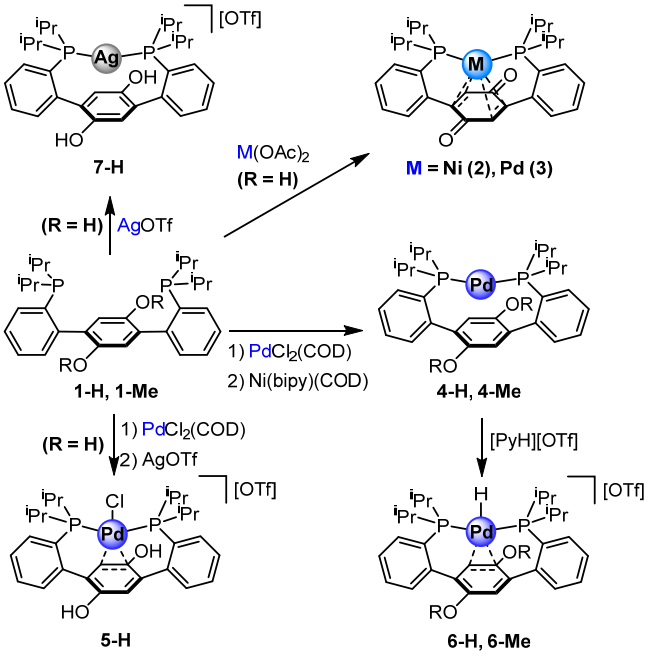

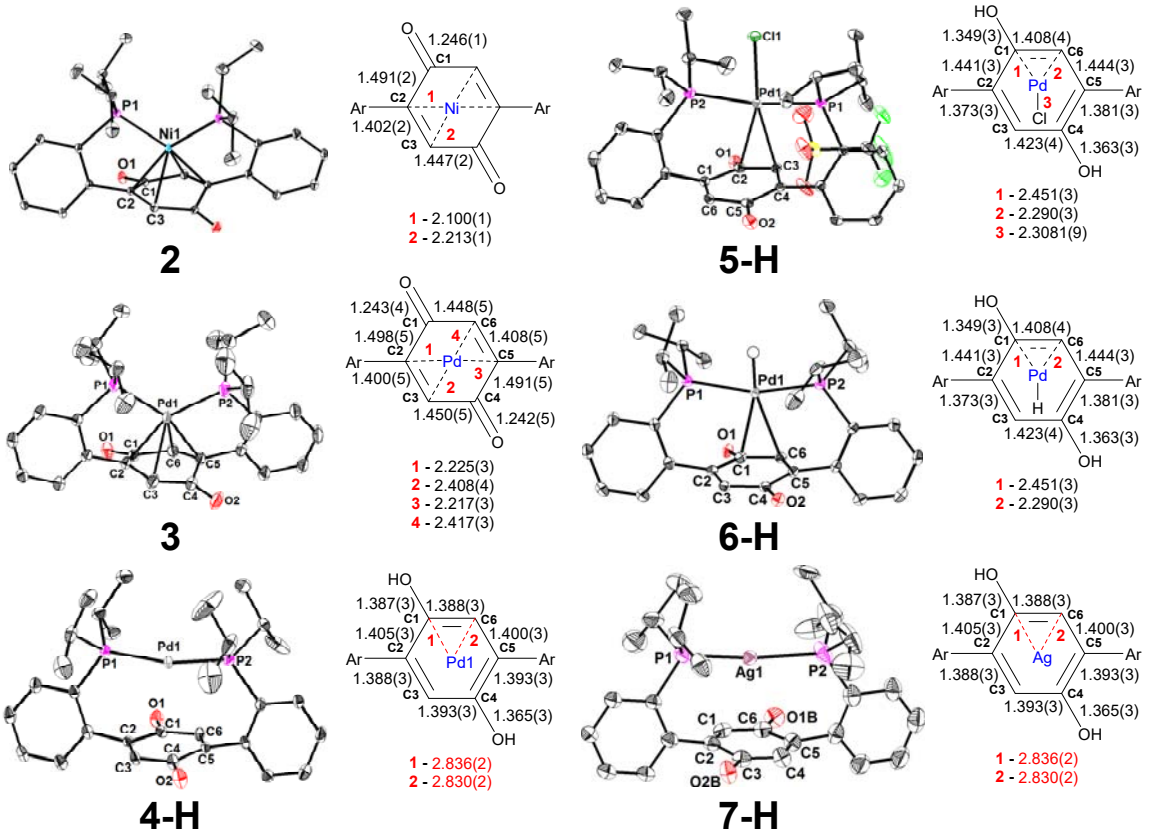

Figure 1. Solid-state structures and selected bond distances for complexes **2**, **3**, **4-H**, **5-H**, **6-H**, and **7-H** (top to bottom). Cocrystallized solvent, counteranions, and most hydrogen atoms omitted for clarity. Bond lengths highlighted in red are too long to represent substantial interactions. Disorder of the hydroquinone oxygen positions has been omitted for clarity for complexes **6-H** and **7-H**.

Single crystal X-ray diffraction (XRD) studies of **2** and **3** (Figure 1) confirm short C-O distances (**2**: 1.246(1) Å; **3**: 1.243(4) 1.242(5) Å) consistent with the quinone assignment for the central arene. Both complex **2** and **3** bind the quinone moiety in an η^4 fashion similar to previously reported metal-quinone complexes.[13a-c, 15] While η^4 binding has precedent for Pd, it should be noted that the majority Pd-quinone structures show η^2 coordination.[13c-e, 15b, 16] Both complex **2** and **3** display a distorted tetrahedral geometry with similar τ_4' values of 0.54 and 0.55 respectively using the two phosphine donors and the centroids of the coordinated C–C double bonds as the ligand contacts. Strong metal-arene interactions are evident from short

average M–C distances of 2.16 and 2.32 Å for **2** and **3** respectively. Substantial backbonding into the quinone C–C double bonds is also evident from the elongated C–C distances of 1.402(2) Å for **2** and 1.400(5) and 1.408(5) Å for **3**. A deplanarization of the quinone moiety is also observed with a C1-(C2-C3-C5-C6 centroid)-C4 angle of 162.2° for **3** and 160.2 ° for the analogous angle in **2**.

Cyclic voltammetry (CV) studies of **2** and **3** in THF were also pursued to establish the redox chemistry of π-bound quinone moiety. Free quinone in DMSO shows two reductions to the corresponding radical anion and the closed shell dianion at -0.91 V and -1.71 V versus Fc/Fc^{+}.[4c] Complex **2** shows a quasireversible reduction event centered at -1.59 V, possibly a two-electron process, and an irreversible oxidation event at 0.77 V versus Fc/Fc^{+} (Figure 2). Complex **3** shows a more complicated CV data with two quasireversible reductions centered at -1.97 and -1.68 V and an irreversible oxidation at 0.54 v versus Fc/Fc^{+} (Figure 3). However, additional oxidation events are observed at -1.09 and -0.4 V corresponding to the reduction events suggesting the formation of multiple species upon two-electron reduction of **3**. Literature electrochemical data for Pd complexes with quinonoid moieties incorporated into the ligand scaffold show reductions at far milder potentials suggesting that the direct coordination of Ni or Pd to the quinone π-system results in significant changes in the electronic properties of the ligand.[9b, 9d, 9e]

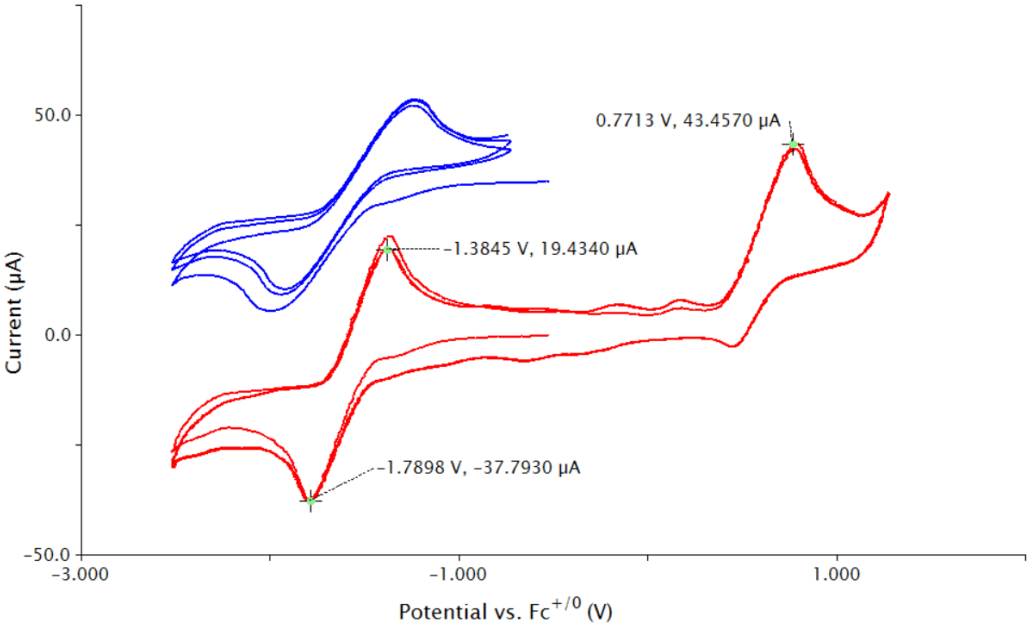

Figure 2. Cyclic voltammetry data for complex **2**.

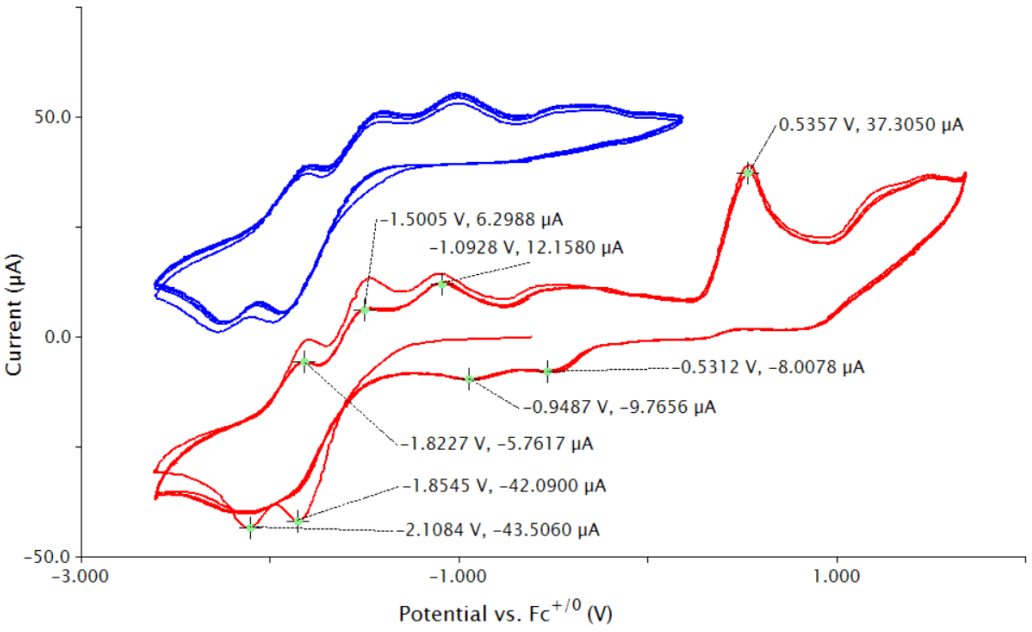

Figure 3. Cyclic voltammetry data for complex **3**.

Efforts to regenerate the hydroquinone form of the central arene by reduction of the quinone in **3** directly was attempted. Conceptually, this transformation corresponds to the delivery of two protons and electrons to the central quinone moiety (Scheme 3), which can be

accomplished with dihydrogen (Pathway 1), discrete sources of protons and electrons (Pathway 2), or through the successive delivery of two hydrogen atoms (Pathway 3).

Scheme 3. Summary of reduction attempts of **3**

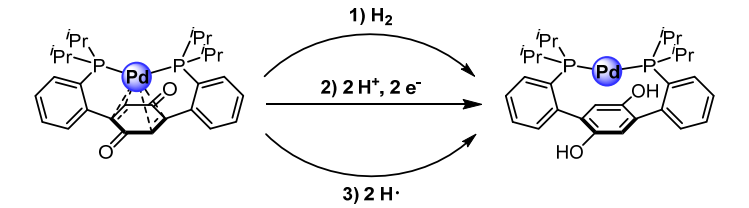

Pathway 1	Pathway 2	Pathway 3
-No direct reaction of 3 with dihydrogen -External catalyst required -Pd/C or Pt/C most selective -Inconsistent scale up	-Electrochemical studies with weak acids looked promising -Stoichiometric studies showed best resuts with KC_8 or sodium napthalenide	-No H-atom transfer from TEMPOH observed -Consistent with BDFE for 1,4-benzoquinone and TEMPOH

Complex **3** proved incapable of rehydrogenating itself with dihydrogen even at elevated temperatures with multiple atmospheres of pressure. The coordinatively saturated nature of the Pd^0 center likely prevents dihydrogen coordination. Furthermore Pdo binding to the π-accepting quinone moiety results in an electron-poor metal center which would disfavor oxidative addition to form a Pd^{II} dihydride. The addition of an external heterogeneous hydrogenation catalyst proved sufficient to generate modest conversions to the desired hydroquinone though some demetalation and other phosphorus-containing species were also observed. Pd/C or Pt/C proved to be the most selective hydrogenation catalysts, however inconsistent results in scale ups were observed with this approach.

The regeneration of the hydroquinone moiety with discrete reductants and acids was also pursued. Given the isolation of stable electrochemical reductions, similar CV studies in the presence of *para-t*Bu benzoic acid were pursued (Figure 4). The addition of acid to complex **3** in cyclic voltammetry experiments resulted in substantial changes in the reductive behavior (Figure 4). An improvement in the chemical reversibility of complex **3** was observed with a

broad quasireversible oxidative (-0.81 V vs Fc/Fc^+) with a very large peak-to-peak separation (1.47 V). The presence of a weak proton source facilitates the reductive and oxidative processes for complex **3** while also substantially improving the potential at which chemical reduction can occur.

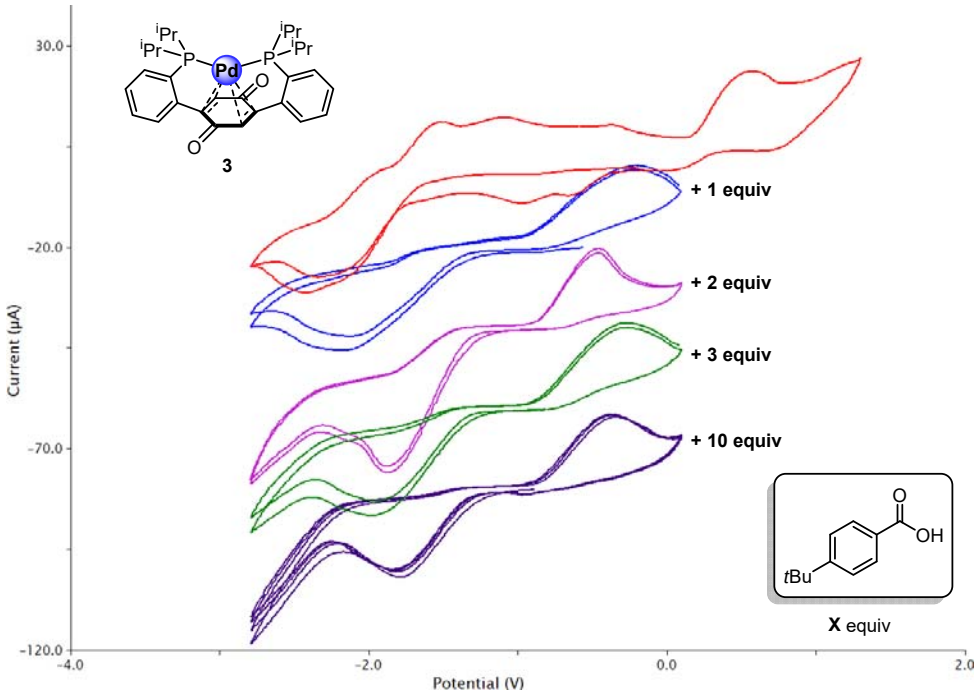

Figure 4. Cyclic voltammetry data for **3** in the presence of varying equivalents of *para-t*Bu benzoic acid.

The obtained CV data suggest strong reductants (~ -1.5 V vs Fc/Fc^+) would still be required for effective reduction of **3** in the presence of two equivalents of *para-t*Bu benzoic acid. No reaction was observed when using Zn^0 or Mg^0 as the reductants. A slow reaction was observed with a Na^0 mirror, however a decomposition product was observed to be the major species by NMR. Kinetically faster reductants were then surveyed and it was found that sodium napthalenide and potassium graphite were capable of a rapid reaction to yield the hydroquinone-Pd^0 complex as the major species. However, removal of naphthalene or other impurities proved challenging due to their similar solubility in hydrocarbon solvents.

Finally, a reaction between complex **3** and 1-hydroxy-2,2,6,6-tetramethyl-piperidine (TEMPOH) (BDFE = 71.0 kcal/mol) was attempted. Unfortunately, no formation of product was observed, which is likely attributable to the weak O–H bond of the first H-atom delivered to 1,4-benzoquinone (65.2 kcal/mol) despite the strength of the first O–H bond in 1,4-hydroquinone (81.5 kcal/mol).

The direct synthesis of Ni^0 and Pd^0 complexes with the hydroquinone form of **1-H** was pursued without using complex **3** as a precursor. Attempted metalations of **1-H** with $Ni(COD)_2$ (COD = 1,5-cyclooctadiene) generated complicated mixtures of species. However, both Pd^0 (**4-H**) and Pd^{II} (**5-H**) species supported by **1-H** proved isolable (Scheme 1). **4-H** was synthesized as brown powder in 84% yield using a one-pot synthesis involving initial metalation with $PdCl_2(COD)$ in THF followed by reduction with Ni(bipy)(COD) (bipy = 2,2'-bipyridine). Treatment of **1-H** with $PdCl_2(COD)$ followed by halide abstraction with silver triflate resulted in the formation of a cationic monochloride species, **5-H**, which could be isolated as a dark red powder in 32% yield. Both **4-H** and **5-H** are stable as solids, but substantial decomposition to a complicated mixture of species in solution is observed over time.

Solution NMR spectra for both **4-H** (C_6D_6) and **5-H** (CD_3CN) show a sharp singlet (**4-H**: 6.94 ppm, **5-H**: 6.72 ppm) and a broad resonance (**4-H**: 4.14 ppm, **5-H**: 8.18 ppm) by ^1H NMR that correspond to the central hydroquinone CH and OH protons, respectively. One methine resonance at 1.88 and 3.12 ppm by ^1H NMR and a sharp singlet at 33.85 and a broad resonance at 34.22 ppm by $^{31}P\{^1H\}$ NMR are observed for **4-H** and **5-H,** respectively. These data are consistent with *pseudo-*C_2 symmetry or fast exchange processes on the NMR time scale. Single crystals suitable for XRD analysis were obtained for **4-H** and **5-H** (Figure 1). Complex **4-H** was found to cocrystallize with a decomposition product where the central arene was

converted to a 2,3-dihydro-1,4-benzoquinone moiety. Formation of this species suggests that decomposition of **4-H** in solution may occur via a metal-mediated isomerization of the hydroquinone moiety. The hydroquinone assignment for the central arene of **4-H** is supported by C–O distances of 1.387(3) and 1.365(3) Å, which are consistent with single bonds. The Pd^0 center in **4-H** is two coordinate as long Pd1–C1 and Pd1–C6 distances of 2.836(2) and 2.830(2) Å respectively represents a negligible metal-arene interaction. Consistent with this assignment, all the C–C bond distances of the central hydroquinone moiety do not vary substantially, ranging between 1.388(3) and 1.405(3) Å and are in line with structures of reported 2,5-diphenyl-1,4-hydroquinone moieties.[17] The P1-Pd1-P2 angle of 165.08(2)° also supports this assignment and is also likely enforced by the *trans*-spanning nature of the rigid *para*-terphenyl framework. These data indicate no disruption of aromaticity is occurring as would be expected upon metal coordination, making the best description of **4-H** a 14 e^-, two-coordinate Pd^0 complex with a spectator hydroquinone moiety.

In complex **5-H**, the C–O bond lengths of 1.349(3) and 1.363(3) Å are comparable to **4-H** and consistent with the hydroquinone assignment for the central arene. Furthermore, complex **5-H** crystallizes with a clear hydrogen bonding interaction between a hydroquinone OH moiety and a neighboring triflate. The Pd^{II} center shows an η^2 interaction with the central arene trans to the Cl ligand with Pd1–C1 and Pd1–C6 distances of 2.451(3) and 2.290(3) Å respectively. Disrupted aromaticity in the hydroquinone moiety is evident from the alternating shorter (C1–C6, C2–C3, C4–C5) and longer (C1–C2, C3–C4, C5–C6) C–C bond lengths which indicate partially localized olefinic character resulting from Pd coordination. The geometry about Pd is square planar with a τ_4' value of 0.10 using the two phosphines, chloride, and centroid of the C1–C6 bond as metal contacts. Complexes **3**, **4-H**, and **5-H** demonstrate

the flexible nature of the Pd-central arene coordination (η^0, η^2, η^4) and how Pd oxidation state (**4-H** to **5-H**) and hydroquinone/quinone interconversion can influence preferred binding modes.

*Section 3.3 Small Molecule Activation by **4-H** and Synthesis of Control Compounds*

Hydroquinone-Pd^0 (**4-H**) and quinone-Pd^0 (**3**) complexes were investigated for reactivity with small molecules toward utilization of protons and electrons stored in the central arene. Clean oxidation of **4-H** to **3** was observed with a variety of gaseous oxidants including dioxygen, nitric oxide, and nitrous oxide, which were all confirmed to produce water as the oxygenic reaction byproduct by ^{1}H NMR spectroscopy when reaction volatiles were transferred between J-Young tubes. 1-azido adamantane was also found to effect the transformation with the formation of 1-amino adamantine confirmed by gas chromatography-mass spectrometry (GC-MS). Additionally, trimethylamine *n*-oxide, 1,4-benzoquinone, and 2,4,6-tri(*tert*butyl)phenoxyl radical were also found to react with **4-H** to form **3**. With all the surveyed small molecule substrates, no further oxidation of **3** was observed.

A more detailed mechanistic understanding of the rapid reactivity of **4-H** with dioxygen was pursued. The reactions of Pd and Pt complexes with molecular dioxygen have been recently reviewed.[18] The direct activation of dioxygen by low-coordinate Pd^0 complexes has been reported and typically yields an η^2-peroxo.[16a, 19] However, a bis-(η^1-superoxo)[20] and a terminal η^1-superoxo[21] have been reported. Therefore it is possible that initial dioxygen activation can occur at the Pd^0 center prior to subsequent activation of the hydroquinone moiety. The reaction of Pd^{II} hydrides with dioxygen to yield hydroperoxo complexes has also been reported though the reaction mechanism varies with different supporting ligands.[6a, 8, 22] Therefore, the possibility of proton transfer to the Pd center from the hydroquinone moiety

prior to dioxygen activation must also be considered. The autooxidation of some hydroquinones by dioxygen in the absence of catalyst has been reported, most notably in the anthraquinone process which is the primary means of industrial hydrogen peroxide production.[23] As a net change in Pd oxidation state does not occur in the conversion of **4-H** to **3**, it is possible that the reaction with dioxygen is entirely mediated by the ligand without involvement of the metal center. Previous studies with a related catechol diphosphine ligand have shown that dioxygen activation likely occurs by an initial outer sphere electron transfer step offering another mechanistic proposal.[11c] Cooperative activation of dioxygen by both Pd center and the ligand in a concerted process is also plausible.

In order to address the aforementioned mechanistic possibilities, suitable complexes to investigate different reactivity patterns were synthesized. To test for Pd-only initial dioxygen activation, a Pd^0 complex supported by a previously reported diphosphine ligand with a para-dimethoxy substituted central arene was synthesized (**4-Me**, see section 2.1 for detailed synthesis) using the same synthetic route as **4-H** with the product obtained as an orange solid in 98% yield (Scheme 1). Solution NMR data (C_6D_6) are consistent with *pseudo*-C_2 symmetry or a fast exchange processes on the NMR time scale with chemical shifts comparable to **4-H**. Sharp singlets are observed for the central arene CH and OMe proton resonances at 6.86 and 3.49 ppm respectively. One methine resonance at 1.96 ppm by ^{1}H NMR and a sharp singlet at 33.81 by $^{31}P\{^1H\}$ NMR are also seen.

To test for the potential reactivity of Pd-H species, complex **4-H** and **4-Me** were protonated with one equivalent of pyridinium triflate to yield **6-H** and **6-Me** respectively (Scheme 1). Solution NMR data for both species (CD_3CN) are quite similar and consistent with *pseudo*-C_2 symmetry or fast exchange processes on the NMR time scale. Reminiscent of **5-H**, the central arene CH proton resonances appear as sharp singlets at 6.79 and 6.99 ppm

for **6-H** and **6-Me,** respectively. The OH and OMe protons appear as a broad resonance at 7.42 and a sharp singlet at 3.73 ppm, respectively. A single methine proton resonance is observed (**6-H**: 2.46 ppm; **6-Me:** 2.48 ppm). Both complexes coincidentally show the Pd–H resonances as a triplets (**6-H**: J_{PH} = 8.5 Hz, **6-Me**: J_{PH} = 9.0 Hz) at -16.33 ppm, while the $^{31}P\{^{1}H\}$ NMR shows a doublet centered at 41.57 ppm for **6-H** and a broadened singlet at 41.93 ppm for **6-Me**.

Single crystals suitable for XRD analysis were obtained for **6-H** (Figure 1). The hydroquinone oxygens were nearly equivalently disordered across the C1/C4 and C3/C6 positions, only the majority species has been shown in Figure 1 for clarity. While this disorder precludes assessment of the C–O bond lengths, the central arene bond distances show an alternation of long and short distances analogous to **4-H** suggestive of disrupted aromaticity in a hydroquinone moiety rather than a quinone assignment. The Pd-center shows η^2 coordination to C1–C6 akin to **5-H** though the Pd1–C1 and Pd1–C6 distances are longer at 2.501(4) and 2.477(3) Å respectively. **6-H** and **6-Me** are cationic and therefore represent a Pd-H that could potentially arise from intermolecular proton transfer between equivalents of **4-H**. These complexes will provide insight into the behavior of Pd–H species on the current ligand platforms and probe how the non-innocence of the hydroquinone moiety affects reactivity. An alternative Pd-H accessible from **4-H** could be neutral, corresponding to (formal) intramolecular proton transfer from the hydroquinone moiety to the Pd center. Such a compound has not been observed or isolated to date.

To probe for ligand-only reactivity, a Ag^{I} complex, **7-H**, was synthesized by metalation of **1-H** with silver triflate in THF. The product was isolated as colorless needles in 68% yield following recrystallization. Solution NMR data (CD_3CN) is consistent with *pseudo*-C_2 symmetry

or a fast exchange process on the NMR time scale. The central hydroquinone OH and CH proton resonances appear as a broad singlet at 6.98 ppm and a sharp singlet at 6.85 ppm respectively. Additionally, a single methine resonance at 2.52 ppm is observed. The $^{31}P\{^{1}H\}$ NMR shows two pairs of doublets centered at 28.33 with J_{PAg} values of 559.7 and 484.9 Hz owing to coupling to ^{107}Ag (52% abundance) and ^{109}Ag (48% abundance) nuclei.

Single crystals of **7-H** suitable for XRD analysis were obtained. Like **6-H**, nearly equivalent disorder of the hydroquinone oxygens is present precluding detailed analysis of the C–O bond lengths. Ag1-C1 and Ag1-C6 distances are in excess of 2.9 Å consistent with a negligible metal-arene interaction similar to that of **4-H**. C–C bond lengths in the hydroquinone moiety do no show an alternation of longer and shorter bond distances. This structural information indicates that **7-H** serves as a suitable electronic and structural control for dioxygen reactivity with the hydroquinone moiety, as no substantial metal-arene interaction perturbs the reactivity of the central arene moiety as seen in **4-H**.

Section 3.4 Studies of Initial Dioxygen Activation

The reactivity of dioxygen with all control compounds was pursued (Scheme 4). At room temperature **4-Me** was found to rapidly react with dioxygen to form a complicated mixture of species. This reactivity differs from that of previously reported bis(phosphine) Pd^0 complexes which are known to form (η^2-peroxo) complexes stable enough to be structurally characterized.[19a, 19b, 19f, 19l, 19q] Compound **7-H** showed no reaction for multiple weeks at room temperature when exposed to one atmosphere of dioxygen (Scheme 3). This indicates that direct oxidation of the hydroquinone moiety of the ligand by dioxygen is not a facile reaction pathway and it likely does not occur in the reaction of **4-H**. Compound **6-H** showed a color change upon mixing to generate a bright pink species that shows a peak at λ_{max} = 520 nm. By

$^{31}P\{^{1}H\}$ and ^{1}H spectroscopy, the starting material is consumed within 6 hours, resulting in the formation of a new major species, **3(H)$^{+}$**. No peaks are observed upfield of 0 ppm, suggesting the lack of a Pd-H moiety. An identical UV/Vis spectrum was obtained upon addition of one equivalent of pyridinium triflate to **3** in THF leading to the assignment of this product as the protonated quinone species. **6-Me** showed reaction with dioxygen upon mixing at room temperature to generate a complicated mixture of species. To test for the direct oxidation of the hydroquinone moiety in **6-H** by dioxygen, **5-H** was treated with O_2, since dioxygen activation across Pd^{II}-Cl bond has not been reported to the best of our knowledge. No reaction with dioxygen was observed for complex **5-H**. Similar to **7-H**, these results suggest that oxidation of the hydroquinone moiety to the corresponding quinone is likely metal-mediated as no evidence for direct ligand chemistry has been seen.

Studies of dioxygen reactivity at lower temperatures were pursued to detect intermediates for mechanistic insight. Dioxygen addition to **4-H** at -78 °C resulted in the formation of a new species (**Int1**, Scheme 5, a) by $^{31}P\{^{1}H\}$ NMR (THF). **Int1** shows two coupling doublets 35.38 and 30.77 ppm (J_{PP} = 32 Hz) consistent with an asymmetric species in solution (Scheme 5, c). Low temperature solution IR data showed no absorptions consistent with a C–O double bond, indicating that no conversion of the hydroquinone moiety to a quinone or semiquinone form had occurred. While observed to be stable at -78 °C for up to an hour, **Int1** was found to be quite thermally sensitive with 80% conversion to **3** occurring at -50 °C over an hour. These data suggest that a Pd-only binding and activation of dioxygen is occurring at lower temperatures without any participation of the hydroquinone.

Scheme 4. Summary of room temperature reactivity

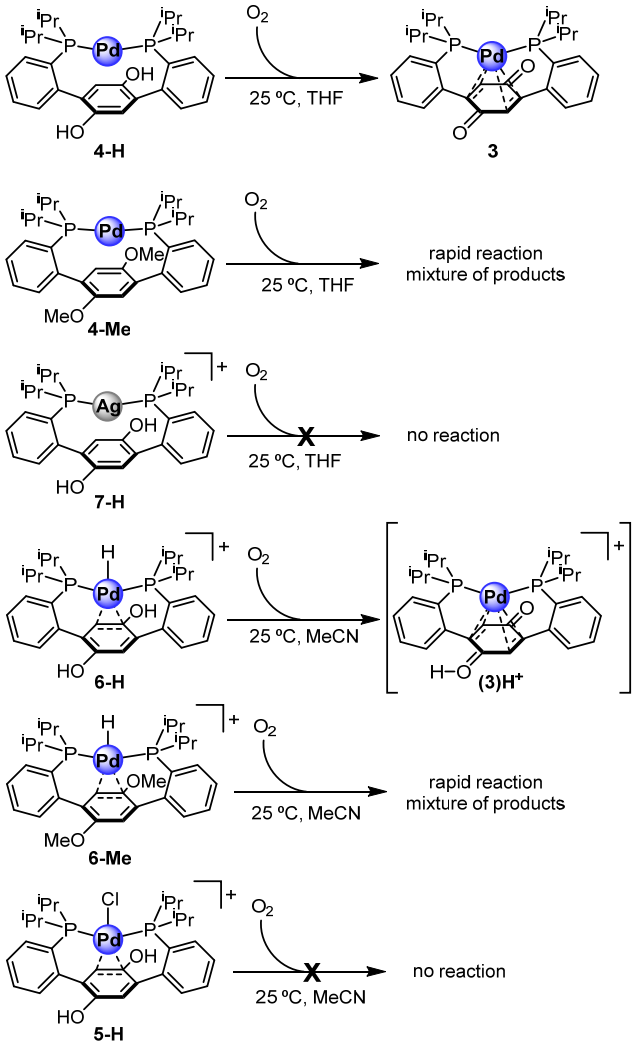

To test if the hydroquinone moiety was necessary for initial activation, dioxygen was added to a solution of **4-Me** at -78 °C, in which the phenolic moieties are protected with methyl groups (Scheme 5, b). The formation of a new species, **8-Me**, was observed upon mixing by NMR (d_8-THF) (Scheme 5, c). Similar to **Int1**, $^{31}P\{^1H\}$ NMR shows two coupling doublets at 34.04 and 29.87 ppm (J_{PP} = 24.0 Hz) again consistent with an asymmetric species suggesting the formation of a very similar species by NMR. By ^1H NMR, two signals for the central arene CH (6.87 and 6.66 ppm) and OMe (3.56 and 3.47 ppm) protons are observed. Three distinct methine proton signals that integrate 1:1:2 appear at 3.67, 3.59, and 1.98 ppm). Unlike **Int1**, **8-**

Me was found to be stable for over four weeks at -78 °C in THF and for over multiple hours at -40 °C with no sign of decomposition. This information further supports the assignment of direct dioxygen binding at the Pd^0 center without involvement of the hydroquinone moiety. Furthermore, the increased stability of **8-Me** suggests that the hydroquinone moiety, when present, facilitates further reactivity with the Pd-coordinated O_2 moiety.

Scheme 5. Proposed dioxygen activation mechanism for **4-H** and **4-Me**

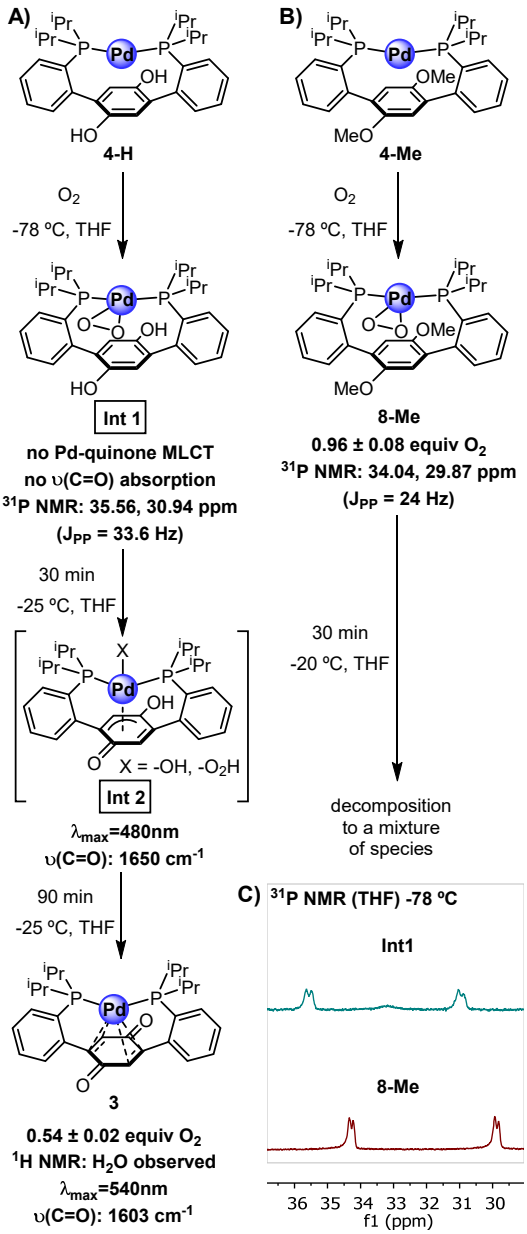

No reaction of **6-H** or **6-Me** with dioxygen was observed at -30 °C by $^{31}P\{^{1}H\}$ NMR (CD_3CN), suggesting that the activation of dioxygen by **4-H** likely does not occur via a cationic Pd-H species. However, reactivity from a neutral complex generated by intramolecular protonation to form a Pd-H moiety and deprotonated hydroquinone cannot be ruled out. The similarity of **Int1** and **8-Me** by NMR further suggests that the activation of dioxygen by **4-H** does not occur via a Pd-H species, given that the precursor to **8-Me** does not have acidic protons. Gas quantification experiments using a Toepler pump was used to determine the equivalents of dioxygen consumed by each reaction (Table 1). At 25 °C, **4-H** and **6-H** were found to consume 0.54 ± 0.02 and 0.95 ± 0.04 equivalents of dioxygen, respectively. Oxygen addition to **4-Me** at -78 °C showed consumption of 0.96 ± 0.08 equivalents of dioxygen. During the freeze-pump-thaw cycles of **Int1** during Toepler pump experiments a noticeable purple hue developed in the reaction vessel indicating the partial formation of **3** regardless of attempts to keep reaction mixtures from warming up substantially. These experiments with **4-H** were likely unsuccessful due to the decreased thermal stability of **Int1** compared to **8-Me** as seen in NMR experiments.

The binding of a single equivalent of dioxygen to **4-Me** at low temperatures rules out the formation of a bis-(η^1-superoxo) (Scheme 6, a). The literature example of a η^1-(superoxo) complex was observed to convert to the corresponding η^2-peroxo over 80 minutes at temperatures above -82 °C.[21] Therefore, the most plausible assignment for **8-Me** and, due to similarities by $^{31}P\{^{1}H\}$ NMR, **Int1**, is an η^2-peroxo species (Scheme 6, a).[24] Furthermore, η^1-(superoxo) would be expected to bind the oxygenic ligand in a position *trans* to the central arene moiety as seen in the case of **5-Cl** resulting in equivalent phosphine donors on the NMR time scale. Differences in reaction rates at low temperature and the amount of dioxygen consumed make reactivity derived from a Pd-H species less likely (Scheme 6, b). The absence

of oxidation of **7-H** rules out hydroquinone oxidation akin to that of the anthraquinone process (Scheme 6, c).[23] It is also noteworthy that the reactivity appears to proceed through an initial inner sphere intermediate unlike previous reports on molybdenum carbonyl complexes (Scheme 6, d). Finally, cooperative activation of dioxygen between the Pd center and hydroquinone ligand is also ruled out as no evidence for hydroquinone oxidation by IR was observed for **Int1**. Additionally, the same type of intermediate can be accessed with **4-Me** which does not have the ability to transfer protons / H-atoms (Scheme 6, e).

Scheme 6. Possible Dioxygen Activation Mechanisms

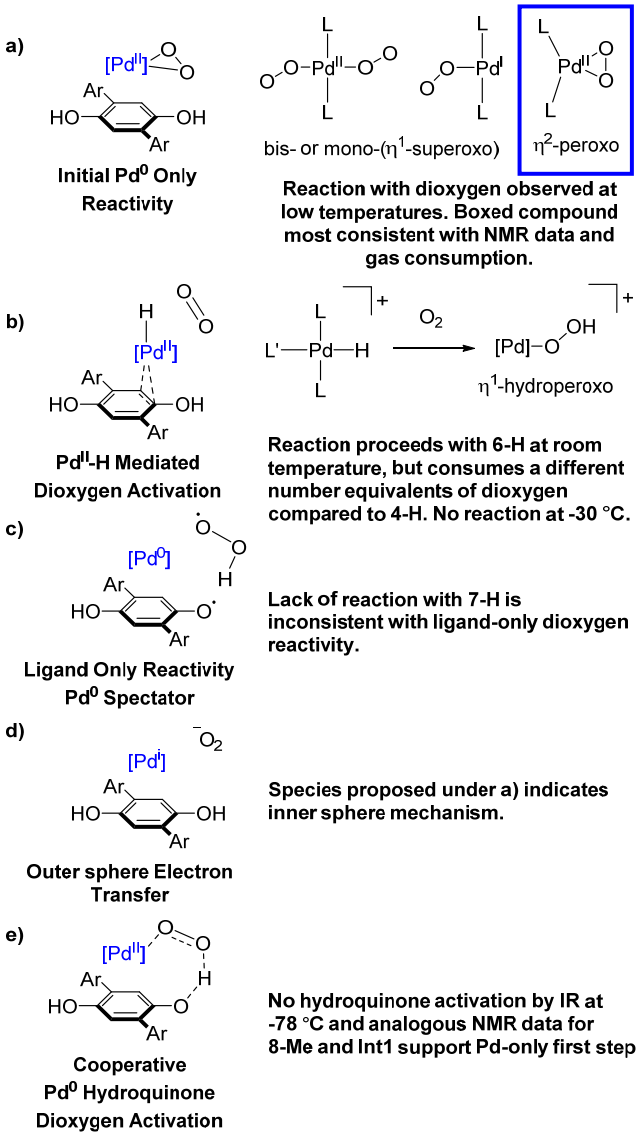

As both **4-H** and **4-Me** activate dioxygen at low temperatures to likely form η^2-peroxo species, the electrophilic or nucleophilic character of the oxygenic moiety of **8-Me** was tested with external substrates. As a test for electrophilic character, **8-Me** was mixed with cyclohexene, 2,4,6-tri*tert*butylphenol, methyl *para*-tolyl sulfide, or triphenylphosphine.[25] No formation of cyclohexanone or sulfoxide product was observed by GC or GC-MS spectroscopy. No formation of 2,4,6-tritertbutylphenoxyl radical was observed by UV/Vis spectroscopy suggesting that an H-atom abstraction pathway is not occurring (BDFE (kcal mol^{-1}) in DMSO: 2,4,6-tri(*tert*butyl)phenol = 80.6, 1,4-hydroquinone = 80.0).[4c] The formation of triphenylphosphine oxide was detected by GC-MS. However low temperature NMR experiments show this reaction to proceed by initial triphenylphosphine substitution of **1-Me** to form $(PPh_3)_2Pd(\eta^2\text{-}O_2)$ by comparison to literature $^{31}P\{^1H\}$ chemical shifts[18a] and independent synthesis from $Pd(PPh_3)_4$ and dioxygen (Figure 22). Subsequent phosphine oxidation therefore likely does not involve terphenyl diphosphine. As a test for nucleophilic character, cyclohexane carboxyaldehyde or *para*-trifluoromethyl benzylalcohol were added to **8-Me**.[25a, 25b] In both cases oxidation products, cyclohexene and the corresponding benzaldehyde, were observed by GC and GC-MS analysis respectively, suggesting nucleophilic character for **8-Me**. These data taken together with the control reactions indicate that dioxygen activation at **4-H** occurs through a Pd-only mediated formation of a (η^2-peroxo) species with nucleophilic character. Hydroquinone activation occurs subsequently through an inter- or intramolecular proton transfer.

Low temperature NMR experiments were run to probe whether both intermolecular proton transfer occur. First, intermolecular proton transfer was tested by studying the reaction of dioxygen with a mixture of **4-Me** and the Ag^I complex, **7-H** (Figure 23). At -78 in THF, **8-Me** was formed in the presence of **7-H** upon the addition of dioxygen. Warming the

reaction mixture to -40 °C did not result in any detectable reaction over more than 30 minutes suggesting intermolecular proton transfer is not occurring at these temperatures. In contrast, **Int1** shows significant conversion over 30 min, even at -50 °C. The dioxygen reactivity of **4-H** in the presence of **7-H** was also tested (Figure 23). As with **4-Me**, oxygen addition at -78 °C in THF resulted in the formation of **Int1** in the presence of **7-H**. Warming the reaction to -40 °C showed near quantitative conversion of **Int1** to form **3** within 10 minutes without any detectable consumption with **7-H**. While these experiments do not rule out intermolecular proton transfer during conversion of **Int1**, they do suggest that such proton transfer to the analogous (η^2-peroxo) species supported by **4-Me** without a pendant hydroquinone moiety either does not occur or is not sufficient for subsequent reactivity of the O_2 moiety.

Oxygen addition at -78 °C to a THF solution of **4-H** resulted in a color change from yellow/brown to orange/brown within thirty seconds consistent with the rapid formation of **Int1** by UV/Vis (Figure 5). Warming the UV/Vis solution of **Int1** to -25 °C resulted in the conversion to a new intermediate (Figure 6), in contrast to the NMR experiments, with a λ_{max} of 480 nm over the course of approximately 30 minutes. This suggests that at lower concentrations, the rates of steps following the formation of **Int1** (and **Int2**) are slowed enough to allow the observation of an additional intermediate. Low temperature solution IR data at -35 °C showed the appearance of an absorption at 1601 cm^{-1} attributable to the formation of a substantial quantity of **3**. However, a small absorption at 1650 cm^{-1} (Figure 18) was also observed that may be attributed to the transient formation of **Int2**, which suggests stepwise activation of the hydroquinone moiety. **Int2** was observed to gradually convert to **3**, the final reaction product, over the course of 3 hours at -25 °C (Figure 7). Cooling the solution of **Int2** to -78 °C could not arrest the conversion to **3**, though the reaction was slower. The formation of **Int2** and **3** both occur with isosbestic points indicating that these

transformations correspond to the clean interconversion of these species. These data show that **Int2** possesses an activated hydroquinone with at least partial quinone character by IR spectroscopy. The UV/Vis spectra of **Int2** is inconsistent with a Pd^{o} protonated quinone, as such structure is assigned to be the product of **6-H** with dioxygen, which can be prepared independently, and shows a peak at λ_{max} = 520 nm. Therefore, it is proposed that **Int2** is a Pd^{II} species with the metal center coordinated to a semiquinone moiety (Scheme 5, a). An anionic oxygenic fragment could be released or still remain coordinated to the metal center in a distorted geometry. If the oxygenic fragment is released, **Int2** would formally correspond to **(3)H**$^{+}$ which is inconsistent with the spectroscopic data. Therefore, it is proposed that an oxygenic moiety remains coordinated, and because of coordination *trans* to the central arene, a second proton transfer is slow allowing observation of this intermediate. As one equivalent of dioxygen is assigned to be bound in **Int1** while only half an equivalent is consumed by the net reaction to **3**, a dioxygen release must occur during the conversion of **Int1** to **3** via an intermolecular disproportionation process. If the oxygen release has already occurred by the time formation of **Int2** then the proposed anionic oxygenic fragment may be a hydroxide ligand. However, if dioxygen release occurs in the conversion of **Int2** to **3**, then the bound oxygenic fragment may be a hydroperoxo species. Unfortunately, the instability of these intermediates and fluorescence from the ligand prevented detailed IR or resonance Raman spectroscopy to further characterize the identity of the reaction intermediates. As intermediate **Int2** is not observed at the higher concentrations of the NMR experiments, the steps following the formation of **Int2** must be slower than its generation. The concentration effect could be a consequence of the intermolecular reaction required for the proposed disproportionation.

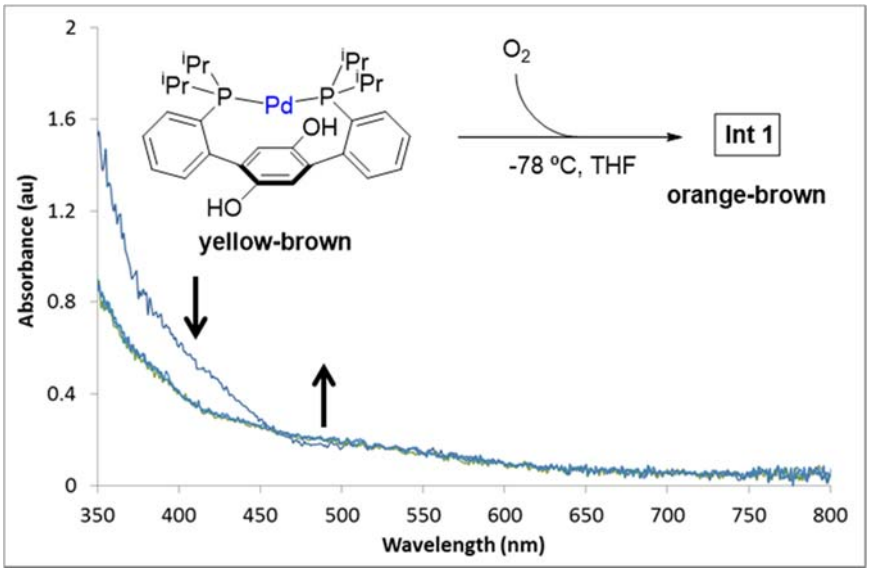

Figure 5. Solution UV/Vis spectrum for **4-H** after warming to -78 °C following O_2 addition.

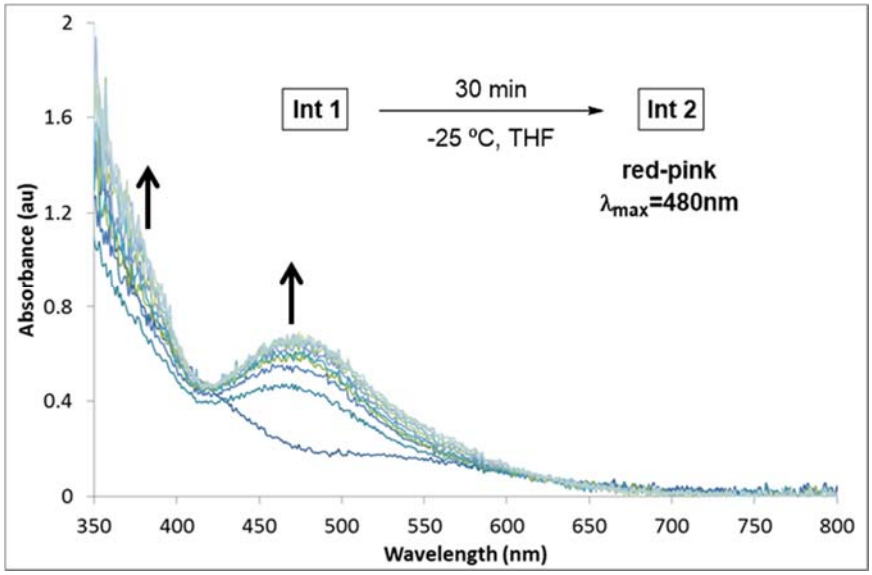

Figure 6. Solution UV/Vis spectrum for **4-H** after warming to -25 °C with O_2 addition over 30 minutes.

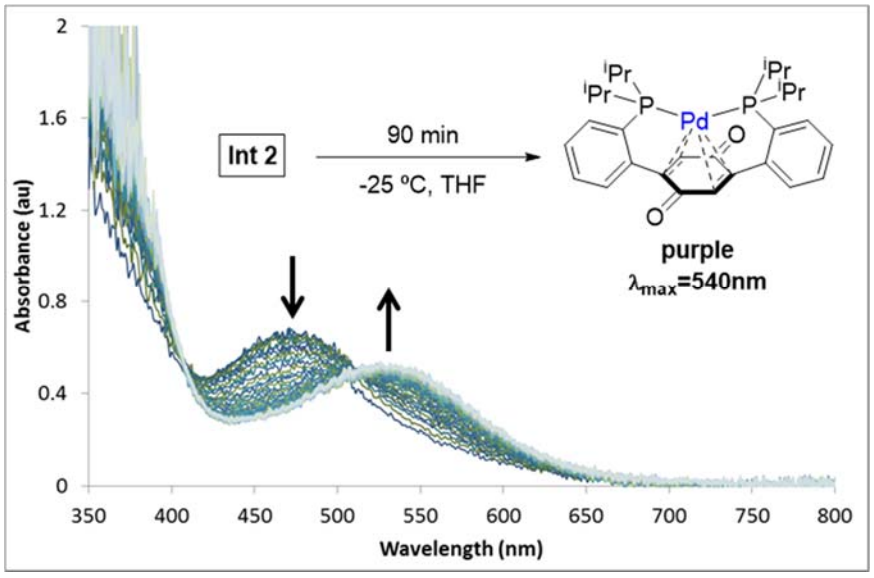

Figure 7. Solution UV/Vis spectrum for the decay of **Int2** at -25 °C over multiple hours.

Kinetics analysis of the conversion of **Int2** into **3** were run to determine the reaction order and gain insight into the reaction mechanism. Two assumptions went into making the calculations: 1) complete conversion to **3** had occurred and 2) the concentration of **Int2** is equal to the final concentration of **3** as inferred from the presence of an isosbestic point. Utilizing the UV/Vis data displayed in Figure 7, and the above assumptions extinction coefficients can be calculated for both **Int2** and **3** at 480 nm and 535 nm. A check of these calculated coefficients were plugged into calculations for the expected summed absorbance values at 480 nm and 535 nm for comparison to experimental data. Good agreement was observed as shown in Figure 8 and Figure 9. This absorbance data was converted into concentrations of **Int1** and **3** using the assumption 2 and plotted (Figure 10) against time. Plotting the natural log of **Int2** concentration against the natural log of time (Figure 11) showed a curved line not consistent with first order process. Plotting the inverse of **Int2** concentration against time (Figure 12) gave a straight line over approximately 120 minutes though noisy data disrupted the fitting of data and greater conversion. However, the linear

regression of the initial 110 minutes (Figure 13) gave an R^2 value of 0.97 suggesting the interconversion of **Int2** and **3** is a second order process.

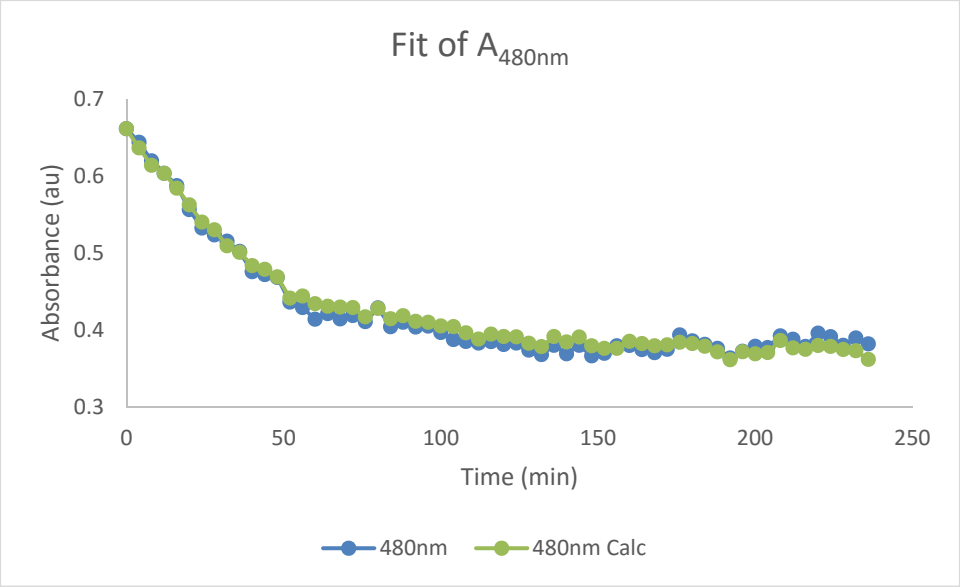

Figure 8. Solution UV/Vis spectrum for the decay of **Int2** at -25 °C over multiple hours.

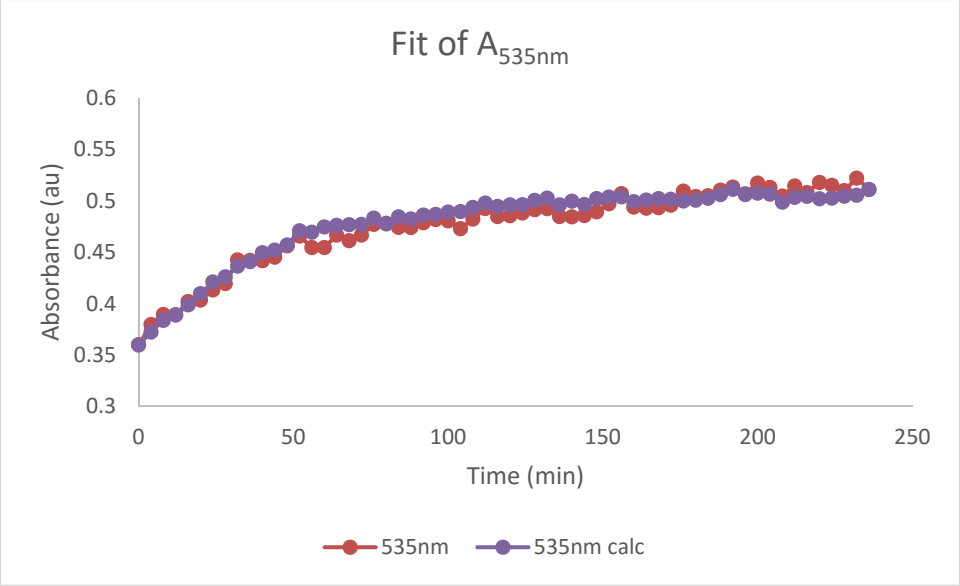

Figure 9. Solution UV/Vis spectrum for the decay of **Int2** at -25 °C over multiple hours.

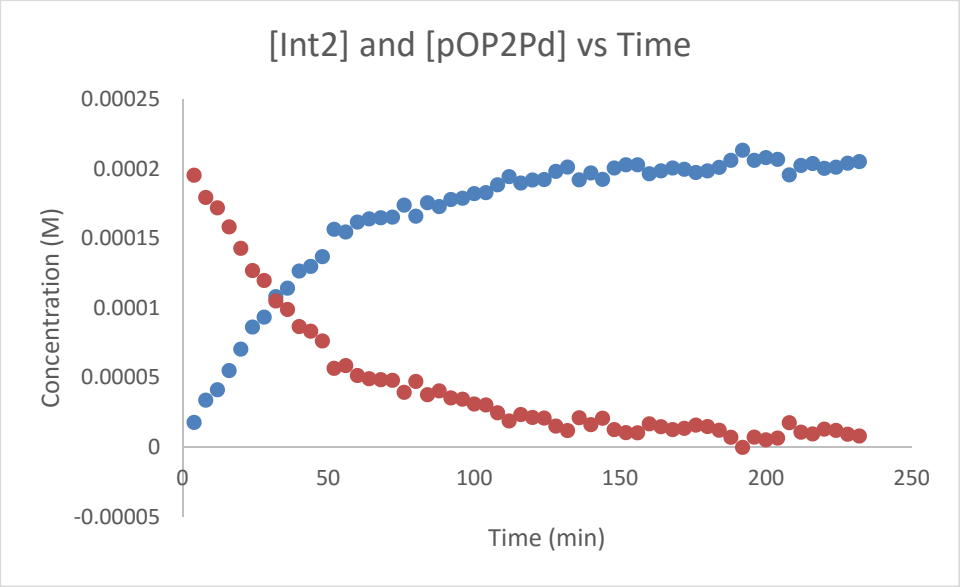

Figure 10. Solution UV/Vis spectrum for the decay of **Int2** at -25 °C over multiple hours.

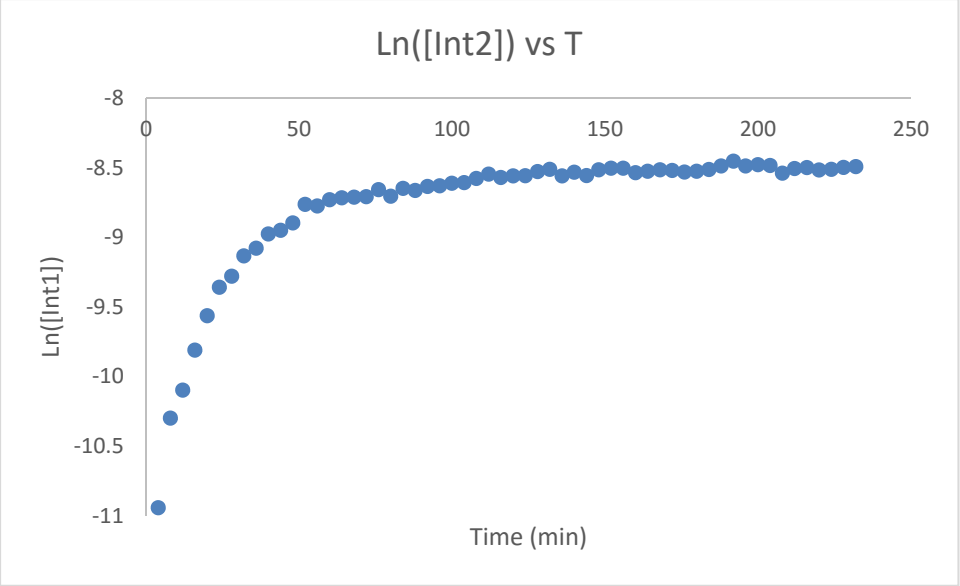

Figure 11. Solution UV/Vis spectrum for the decay of **Int2** at -25 °C over multiple hours.

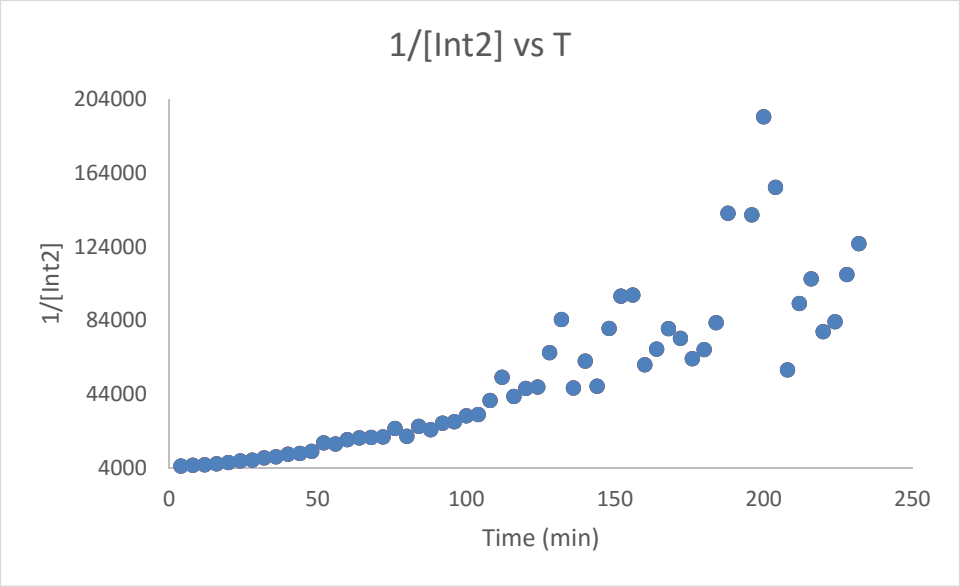

Figure 12. Solution UV/Vis spectrum for the decay of **Int2** at -25 °C over multiple hours.

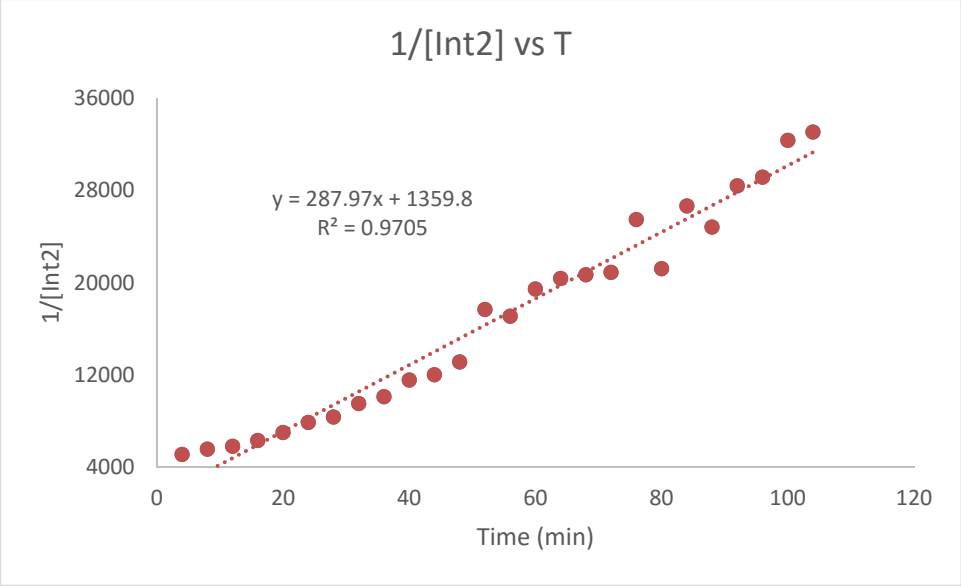

Figure 13. Solution UV/Vis spectrum for the decay of **Int2** at -25 °C over multiple hours.

In catalytic Pd-meditated organic transformations that utilize benzoquinone as a stoichiometric oxidant, the regeneration of $Pd^{II}X_2$ species required for substrate oxidation relies on the transfer of reducing equivalents from Pd^0 to the quinone moiety.[6] Compound **3**

allows investigation of the propensity of a Pd^0 center coordinated to the π-system of the quinone to undergo oxidation or protonation. As supported by CV data and air stability, the oxidation of **3** to form a Pd^{II}-quinone complex requires strong oxidant. Excess (5 equivalents) aqueous hydrogen peroxide was found to slowly bleach the characteristic UV/Vis features of **3** (88% conversion over 12 hours) at room temperature, however well-defined reaction products could not be isolated. The present reactivity suggests that loss of the benzoquinone ligand might be necessary prior to (or in concert with) oxidation of Pd^0, for example with O_2.[6a] In the present system, **4-H** undergoes facile reaction with O_2, showing that upon removal of hydroquinone coordination, oxidation of Pd^0 occurs readily. As Pd^{II}-H species are known intermediates in benzoquinone mediated chemistry, further studies were performed with **6-H**.[6a]

Scheme 7. Proposed Dioxygen Activation Mechanism of **6-H**

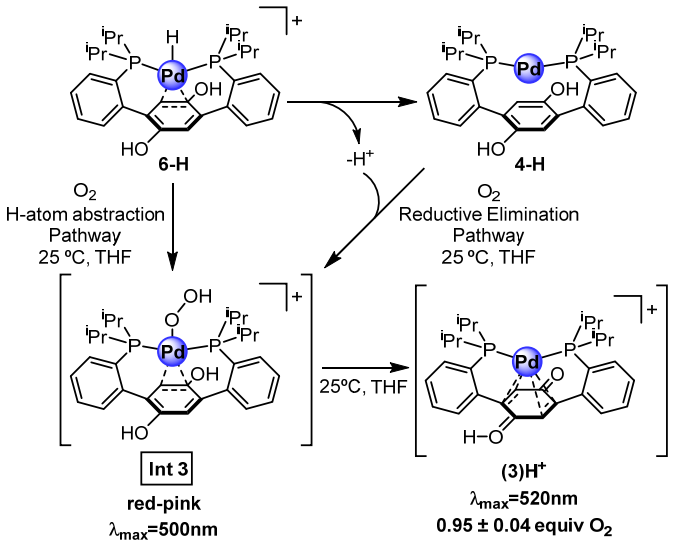

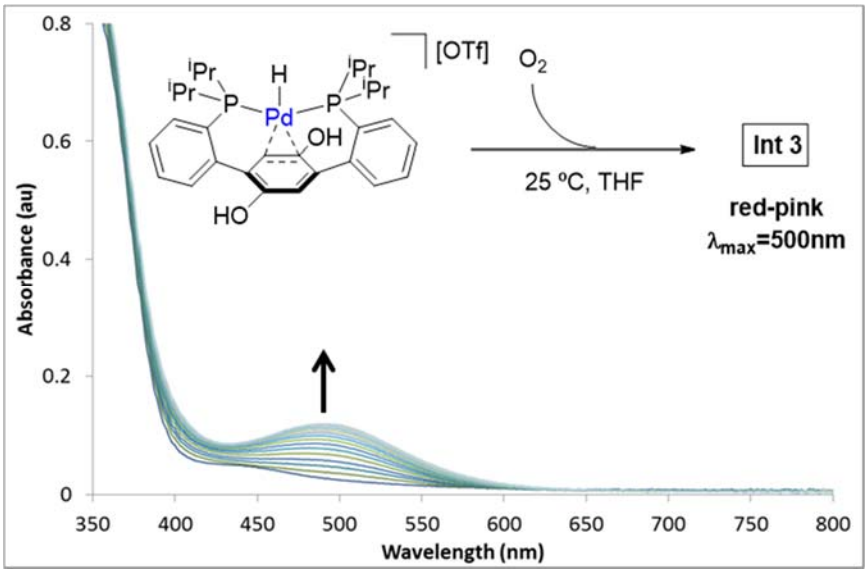

Figure 14. Solution UV/Vis spectrum for **6-H** at 25 °C following O_2 addition over multiple hours.

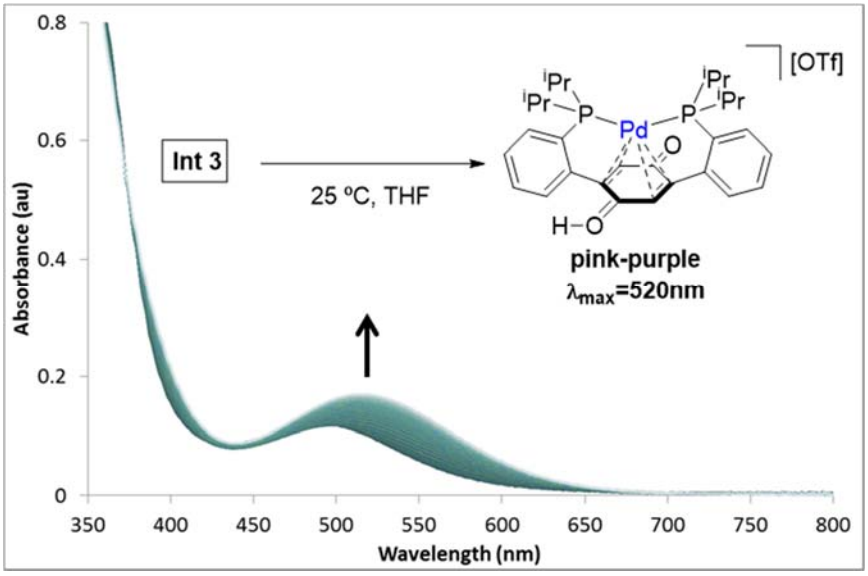

Figure 15. Solution UV/Vis spectrum for the conversion of **Int3** to **(3)H**$^+$ after over multiple 12 hours.

By UV/Vis spectroscopy, **6-H** was found to convert to a pink compound with λ_{max} of 500 nm over several hours following oxygen addition at room temperature (Figure 14). The subsequent conversion to the final product that has a λ_{max} of 520 nm (Figure 15) requires

greater than 16 hours for completion as judged by the slowly shifting λ_{max} in the UV/Vis spectrum. Toepler pump experiments indicate the overall reaction consumes a single equivalent of dioxygen. Based on literature precedence this reaction may proceed via the initial formation of a hydroperoxo species in a geometry akin to **5-H** where the central hydroquinone moiety is *trans* to the oxygenic ligand. Whether this transformation occurs via a reductive elimination / deprotonation route or a hydrogen-atom abstraction pathway as proposed in the literature is unknown at this point (Scheme 7).[22b, 22c] Subsequent deprotonation of the hydroquinone moiety by the hydroperoxide results in release of H_2O_2 and formal reduction of the metal center by the pendant hydroquinone.[26] Given the difference in rate of oxidation between **6-H** and **4-H**, a cationic Pd-H is not an intermediate consistent with the fast reaction of **4-H** with O_2. Previously, benzoquinone has been reported to promote reductive elimination of carboxylic acid from Pd-H complexes.[6a] The final product (**3(H)$^+$**) in the reaction of **6-H** with O_2, lacking diagnostic Pd-H peaks by ^{1}H NMR spectroscopy, indicates that formation of such hydritic species by formal oxidation via protonation at the metal is unfavorable. The π-acidic benzoquinone moiety bound to Pd^0 makes the metal center electron deficient and stabilizes the lower oxidation state.

CONCLUSIONS

A novel non-innocent ligand platform capable of cooperatively mediating the multiproton-multielectron reduction of multiple substrates at a Pd^0 center has been synthesized based on a hydroquinone-diphosphine moiety. Reduction of O_2 was studied in detail. The reaction occurs by an initial Pd-mediated step which involves binding of one equivalent of dioxygen to form a nucleophilic η^2-peroxo species assigned by comparison to complex **8-Me**, displaying a dimethylated hydroquinone moiety. Subsequent activation of the

hydroquinone moiety occurs at higher temperatures with a second intermediate observable by UV/Vis spectroscopy at low concentrations. The reported reactivity represents an overall transformation that requires both the redox active metal capable of binding O_2 as well as the non-innocent pendant hydroquinone within the same molecule. A related Pd^0 complex (**4-Me**), lacking the hydroquinone moiety, or Ag^I-hydroquinone complex (**7-H**), lacking a metal center capable of binding O_2, do not reproduce the reactivity independently or even in combination. Overall, the described results highlight the potential for the reduction of small molecule substrates by utilizing auxiliary redox-active and acid-base non-innocent moieties to store reducing equivalents. From the perspective of oxidation organic methodology utilizing the Pd-benzoquinone combination, O_2 does not react with the isolated Pd^0-benzoquinone species and protonation occurs at the quinone moiety indicating that the oxidized quinonoid moiety prevents reactivity at the coordinated metal.

EXPERIMENTAL SECTION

General considerations.

All air- and/or water-sensitive compounds were manipulated using standard vacuum or Schlenk line techniques or in an inert atmosphere glove box. The solvents for air- and moisture-sensitive reactions were dried over sodium benzophenone ketyl, calcium hydride, or by the method of Grubbs.[27] All NMR solvents were purchased from Cambridge Isotopes Laboratories, Inc. and dried over sodium benzophenone ketyl or calcium hydride. Unless mentioned otherwise, reagents were used as received from commercial suppliers without further purification. Nickel(II)acetate, palladium(II)acetate, chlorodiisopropylphosphine, boron tribromide, silver trifluoromethanesulfonate, 1.7 M *t*BuLi in pentane, diisopropylethylamine, 1,4-dimethoxybenzene, were purchased from Sigma Aldrich. (1,5-cyclooctadiene)palladium(II)chloride, bis(1,5-cyclooctadiene)-Ni(0), tetrakis-(triphenylphosphine)palladium(0), tris-(dibenzylideneacetone)-dipalladium(0), were purchased from Strem Chemicals Inc.Iodine monochloride was purchased from Alfa Aesar. , 2-Bromophenylboronic acid was purchased from Ark Pharm. 2.1 M methyl chloromethyl ether (MOMCl) in toluene,[28] (2,2'-bipyridine)(1,5-cyclooctadiene)nickel(0),[29] 1,4-dimethoxy-2,5-diiodobenzene,[30] 2,5-diiodo-1,4-hydroquinone,[31] and **1-Me**[32] were made according to literature procedures. All ^{1}H, ^{13}C, and ^{31}P spectra were recorded on Varian Mercury 300 MHz, or Varian INOVA-500 or 600 MHz spectrometers at room temperature. Chemical shifts for ^{1}H and ^{13}C NMR data are reported relative to residual solvent peaks.[33] ^{31}P NMR chemical shifts are reported with respect to the deuterated solvent used to lock the instrument. Solution IR spectra were obtained as solution samples using a CaF_2 window cell on a Thermo Scientific Nicolet 6700 FT-IR spectrometer. *In situ* solution IR spectra were recorded on an iC10 ReactIR (Mettler Toledo) equipped with a K4 conduit and a SiComp Sentinel sensor in a

custom-made glass vessel. The UV/Vis spectra were recorded on a Varian Cary Bio 50 spectrophotometer. Low-temperature UV/Vis spectra were obtained using a Varian dip-probe (661.202-UV, 10 mm) and custom-made glass vessel. Elemental analyses were performed by Robertson Microlit Laboratories, Ledgewood, NJ.

Synthesis of 2,5-diiodo-1,4-bis(methoxymethylether)hydroquinone (A)

The synthesis of 2,5-diiodo-1,4-bis(methoxymethylether)hydroquinone has been previously reported, however this protocol provides an alternative synthetic route. 2,5-diiodo-1,4-hydroquinone (2 g, 5.53 mmol, 1 equiv) was added to a 3-neck flask under a counterflow of nitrogen. Degassed, anhydrous dichloromethane (100 mL) was then added with a cannula to yield a suspension. Diisopropylethylamine (11.6 mL, 66.3 mmol, 12 equiv) was then added with a syringe and the reaction mixture allowed to stir for 1 minute. Methylchloromethylether was then added (~2.1 M in PhMe, 26.3 mL, 55.3 mmol, 10 equiv) with a syringe and the reaction was allowed to stir for 3-4 hours during which time the solution became homogenous. The reaction was monitored by GC-MS until all starting material was consumed. The reaction mixture was then washed with a saturated sodium bicarbonate solution. The organic layer was then collected and dried with magnesium sulfate before volatiles were removed by rotary evaporation to yield the clean product as an off-white residue. Characterization matched previous literature reports. Yield: 2.07 g (83 %).

Synthesis of 2,5-bis(2-bromophenyl)-1,4-(methoxymethylether)hydroquinone (B)

The Suzuki coupling to produce the terphenyl product was run as a modification of literature procedure.[34] A Schlenk tube fitted with a Teflon stopper was charged with 2,5-diiodo-1,4-bis(methoxymethylether)hydroquinone (500 mg, 1.11 mmol, 1 equiv.), 2-bromophenylboronic acid (468.6 mg, 2.33 mmol, 2.1 equiv.), and K_2CO_3 (921.3 mg, 6.67 mmol, 6 equiv.). Toluene (26 mL), ethanol (6 mL), and water (6 mL) were then transferred to the Schlenk tube along with a magnetic stirbar. The mixture was degassed by two freeze pump thaw cycles and then put under positive nitrogen pressure. Under a strong counterflow of nitrogen, $Pd(PPh_3)_4$ (64.2 mg, 0.056 mmol, 0.05 equiv.) was added and the solution became a pale yellow color. The reaction mixture was then heated to 65 ºC and stirred for 16-24 hrs while monitoring the reaction by GC-MS. The volatiles were then removed on a rotovap and the residue extracted using dichloromethane and water. The organic layer was then collected and dried using magnesium sulfate before volatiles were removed on a rotovap. Following recrystallation from dichloromethane-methanol the product was obtained as off-white crystalline powder. Yield: 400 mg (71 %). ^{1}H NMR (500 MHz, $CDCl_3$) δ 7.67 (d, J_{HH} = 8.0 Hz, Ar*H*, 2H), 7.37 (m, Ar*H*, 4H), 7.25 – 7.20 (m, Ar*H*, 2H), 7.06 (s, central-Ar*H*, 2H), 5.02 (broad s, OC*H*$_2$O, 4H), 3.33 (s, OC*H*$_3$, 6H). ^{13}C NMR (126 MHz, $CDCl_3$) δ 149.23 (s), 139.54 (s), 132.68 (s), 132.17 (broad s), 131.93 (s), 129.00 (s), 127.11 (s), 124.21 (s), 118.74 (s), 96.14 (s), 56.20 (s). GC-MS (m/z): Calcd, 508.0 (M^+). Found: 508.0 (M^+), FAB-MS (m/z): Calcd, 506.9630 (M+). Found: 506.9623 (M^+).

Synthesis of 2,5-bis(2-(diisopropylphosphino)phenyl)-1,4-hydroquinone (1-H)

Phosphination run as a modification of literature procedures. A Schlenk tube fitted with a screw-in Telfon stopper was charged with 2,5-bis(2-bromophenyl)-1,4-bis(methoxymethylether)hydroquinone (1 g, 1.96 mmol, 1 equiv.) and a magnetic stirbar. Tetrahydrofuran (60 mL) was then to the Schlenk tube. The reaction was cooled to -78 ºC and *tert*-butyllithium (1.7 M pentane solution, 5.4 mL, 8.07 mmol, 4.1 equiv.) was added while stirring to generate a pale yellow solution. The reaction mixture was allowed to warm to room temperature and then stirred for an additional hour. During this time the solution became a cloudy suspension. Chlorodiisopropyl phosphine (0.656 mL, 4.13 mmol, 2.1 equiv.) was then added to the reaction via syringe. The solution immediately became a homogenous pale yellow solution which was allowed to stir for 16 hours. The volatiles were then removed under reduced pressure on the Schlenk line. Acidified methanol (13 mL concentrated HCl, 60 mL MeOH) was quickly degassed on the Schlenk line and then cannula transferred to the dried reaction residue which formed a pale yellow homogeneous solution. The reaction mixture was allowed to stir for 4 hrs at 70 °C to ensure complete removal of the methoxymethylether protecting group before all volatiles were removed under reduced pressure. The reaction was then brought into a wet inert atmosphere glovebox and extracted with dichloromethane. The organic layer was washed with saturated aqueous potassium carbonate followed by saturated ammonium chloride. The organic layer was then dried over magnesium sulfate and the volatiles were then removed under reduced pressure. After drying the residue overnight with heating to 60 °C the reaction was then brought into the dry inert atmosphere glovebox. The residue was washed with cold pentanes and then cold ether to yield the pure product as an off-white solid. Yield: 460 mg (47 %). ^{1}H NMR spectra of product is broad at room temperature due to hindered rotation around aryl–aryl bonds. This is corroborated by ^{31}P

NMR where two distinct peaks are observed at room temperature. ^{1}H NMR (300 MHz, C_6D_6) δ 7.22 (broad s, Ar*H*, 4H), 7.05 (broad s, Ar*H*, 4H), 5.78 (broad s, O*H*, 1H), 5.42 (broad s, O*H*, 1H), 1.93 (broad s, C*H*, 2H), 1.71 (broad s, C*H,* 2H), 0.84 (unresolved m, C*H₃*, 24H). ^{13}C{^{1}H} NMR (126 MHz, C_6D_6) δ 145.76 (s), 134.38 (d, J_{PC} = 45.8 Hz), 131.94 (s), 129.24 (s), 127.01 (s), 121.76 (s), 120.72 (s), 25.35 (s), 21.97 (s), 21.33 (s), 19.89 (s), 19.27 (s), 18.18 (s). At room temperature, **1** shows two distinct ^{31}P NMR signals due to hindered rotation around the aryl-aryl bonds. ^{31}P{^{1}H} NMR (121 MHz, C_6D_6) δ 1.80 (s), -0.06 (s). FAB-MS (m/z): Calcd: 495.2578 (M^+). Found: 495.2582 (M^+).

Synthesis of Complex 2

Compound **1-H** (100 mg, 0.202 mmol, 1 equiv.) was dissolved in tetrahydrofuran (6 mL) and transferred to a Schlenk tube fitted with a screw-in Teflon stopper. $Ni(OAc)_2$ (35.7 mg, 0.202 mmol, 1 equiv.) was suspended in tetrahydrofuran and then added to the solution of **1**. The Schlenk tube was then sealed and heated to 80 °C for 16 hours outside the glovebox during which time to solution became a cloudy green. The reaction mixture was then dried under reduced pressure and brought back into the inert atmosphere glovebox. The crude residue was suspended in diethyl ether and filtered onto a Celite pad. The green solid was washed with additional diethyl ether until the washes became colorless. The product was brought through the Celite pad using tetrahydrofuran. The combined tetrahydrofuran filtrate was dried under reduced pressure to yield the clean product as a green powder. Yield: 65 mg (58 %). ^{1}H NMR (500 MHz, CD_2Cl_2) δ 7.62 (d, J_{HH} = 7.6 Hz, Ar*H*, 2H), 7.58 (t, J_{HH} = 7.4 Hz, Ar*H*, 2H), 7.50 (t, J_{HH} = 6.7 Hz, Ar*H*, 2H), 7.45 (t, J_{HH} = 7.5 Hz, Ar*H*, 2H), 6.16 (s, central Ar*H*, 2H), 2.56 (m, C*H*, 2H), 2.28 (m, C*H*, 2H), 1.32 – 1.24 (m, C*H₃*, 12H), 1.21 (dd, J_{PH} =

16.1 Hz, J_{HH} = 7.0 Hz, C*H₃*, 6H), 1.09 (dd, J_{PH} = 15.8 Hz, J_{HH} = 7.0 Hz, C*H₃*, 6H). $^{13}C\{^1H\}$ NMR (126 MHz, CD_2Cl_2) δ 162.79 (s), 146.43 – 145.62 (m), 138.53 – 136.77 (m), 130.95 (d, J_{PC} = 16.1 Hz), 127.68 (s), 120.33 – 117.76 (m), 96.46 (s), 27.29 (m), 19.99 (s), 17.97 (s), 17.82 (s), 17.43 (s). $^{31}P\{^1H\}$ NMR (121 MHz, CD_2Cl_2) δ 54.30 (s). IR (CaF_2 window, THF, cm^{-1}) ν_{C-O}: 1597. Anal. Calcd. for: $C_{30}H_{38}NiO_2$ (**2)** (%): C, 65.36; H, 6.95. $C_{31}H_{40}Cl_2NiO_2$ (**2•DCM)** (%): C, 58.53; H, 6.34. Found: C, 58.94; H, 6.18.

Synthesis of Complex 3 using $Pd(OAc)_2$

Compound **1-H** (100mg, 0.202 mmol, 1 equiv.) was dissolved in tetrahydrofuran (10 mL) and transferred to a 20 mL scintillation vial. Palladium diacetate (45.4 mg, 0.202 mmol, 1 equiv.) was added as a tetrahydrofuran solution, which in the immediate formation of a deep purple solution. The reaction mixture was allowed to stir for 16 hours before volatiles were removed under reduced pressure to yield a purple residue. The residue was filtered through a Celite pad with tetrahydrofuran. The combined tetrahydrofuran filtrate was dried under reduced pressure to yield the product as a purple powder. Yield: 70 mg (58 %).

Synthesis of Complex 3 using $Pd_2(dba)_3$ and O_2

Compound **1-H** (300 mg, 0.606 mmol, 1 equiv.) was dissolved in tetrahydrofuran (10 mL) and then transferred to a 20 mL scintillation vial. Tris(dibenzylideneacetone dipalladium(0) (277.7 mg, 0.303 mmol, 0.5 equiv.) was then partially dissolved in tetrahydrofuran (10 mL) and added to the solution of **1**. The reaction mixture was allowed to stir for 30 minutes. The scintillation vial was then removed from the inert atmosphere glovebox and exposed to air

and allowed to stir for 1 hour. The reaction immediately turned a deep purple upon exposure to air. The reaction mixture was then poured onto a silica plug that had been wet packed with ethyl acetate (Note: the product is not indefinitely stable on silica and should be eluted quickly from the plug column). Excess dibenzylideneacetone was eluted with ethyl acetate as evidenced by a yellow band. The product was then eluted with methanol taking care to collect only the purple band. The methanol filtrate was then dried under reduced pressure. The purple residue was dried on the Schlenk line overnight and brought into the glovebox where it was dissolved in dry dichloromethane and redried under reduced pressure to yield the product as a purple powder. Yield: 219.7 mg (60 %). ^{1}H NMR (300 MHz, CD_2Cl_2) δ 7.62 – 7.54 (m, Ar*H*, 2H), 7.53 – 7.48 (m, Ar*H*, 4H), 7.47 – 7.37 (m, Ar*H*, 2H), 6.10 (s, central Ar*H*, 2H), 2.46 (dtt, C*H*, 2H), 2.33 (m, C*H*, 2H), 1.13 (m, C*H*$_3$, 24H). ^{13}C{^{1}H} NMR (126 MHz, CD_2Cl_2) δ 165.45 (s), 146.28 – 145.30 (m), 140.90 – 139.75 (m), 132.41 (s), 130.78 (s), 129.82 (s), 128.81 (vt, J_{PC} = 7.9 Hz), 127.82 (d, J_{PC} = 2.5 Hz), 102.64 (s), 28.18 – 27.56 (m), 26.85 – 25.79 (m), 19.38 (t, J_{PC} = 3.7 Hz), 18.70 (vt, J_{PC} = 3.6 Hz), 18.34 (s), 18.05 (s). ^{31}P{^{1}H} NMR (121 MHz, CD_2Cl_2) δ 55.02 (s). IR (CaF_2 window, THF, cm^{-1}) $\nu_{C\text{-}O}$: 1603. Anal. Calcd. for: $C_{30}H_{38}FO_4P_2Pd$ (**3)** (%): C, 60.16; H, 6.39. Anal. Calcd. for: $C_{31}H_{40}Cl_2O_4P_2Pd$ (**3•DCM)** (%): C, 54.44; H, 5.90. Found: C, 54.90; H, 6.00.

Synthesis of Complex 4-H

Compound **1-H** (300 mg, 0.606 mmol, 1 equiv.) was dissolved in tetrahydrofuran (10 mL) and transferred to a Schlenk tube fitted with a screw-in Teflon stopper. (1,5-cyclooctadiene)palladium(II) dichloride (173.2 mg, 0.606 mmol, 1 equiv.) was then added as a partially dissolved suspension in tetrahydrofuran (15 mL). The reaction mixture was allowed

to stir for 2 hours during which time the reaction became a homogeneous orange solution. (1,5-cyclooctadiene)(2,2'-bipyridine)nickel(0) (195.6 mg, 0.606 mmol, 1 equiv.) was then dissolved in tetrahydrofuran (15 mL) and transferred to the reaction mixture. This resulted in an immediate color change to a heterogeneous brown/orange suspension. After stirring for 15 minutes the reaction mixture was filtered through a Celite pad with washing with additional tetrahydrofuran until washes became less colored. The combined tetrahydrofuran filtrate was dried under reduced pressure to yield a brown residue. This residue was then redissolved in benzene and lyophilized to yield the product as a brown powder. Yield: 305 mg (84 %). *Note*: the product is not indefinitely stable in solution and eventually decomposes to a mixture of species. However, it is stable in the solid state. ^{1}H NMR (300 MHz, C_6D_6) δ 7.41 – 7.29 (m, Ar*H*, 4H), 7.12 – 7.03 (m, Ar*H*, 4H), 6.94 (s, central Ar*H*, 2H), 4.14 (s, O*H*, 2H), 1.88 (m, C*H*, 4H), 1.35 (m, C*H*$_3$, 12H), 0.95 (m, C*H*$_3$, 12H). ^{13}C{^{1}H} NMR (126 MHz, C_6D_6) δ 145.26 (s), 144.83 (vt, J_{PC} = 10.2 Hz), 135.02 (vt, J_{PC} = 9.7 Hz), 132.01 (s), 129.67 (s), 128.57 (s), 128.19 (s), 124.22 (s), 29.15 (vt, J_{PC} = 6.1 Hz), 27.82 (vt, J_{PC} = 6.2 Hz), 22.04 (vt, J_{PC} = 8.3 Hz), 21.82 (vt, J_{PC} = 9.1 Hz), 20.80 – 20.30 (m). ^{31}P{^{1}H} NMR (121 MHz, C_6D_6) δ 33.85 (s). Anal. Calcd. for: $C_{30}H_{40}O_2P_2Pd$ (**4)** (%): C, 59.95; H, 6.71. Found: C, 60.21; H, 6.71.

Synthesis of Complex 5-H

Compound **1-H** (100.7 mg, 0.204 mmol, 1 equiv.) was dissolved in tetrahydrofuran (8 mL) and added to a 20 mL scintillation vial containing (1,5-cyclooctadiene)palladium(II) dichloride (58.1 mg, 0.204 mmol, 1 equiv.). The reaction mixture was allowed to stir for 2 hours during which time the solution became a homogeneous orange. Silver triflate (52.3 mg, 0.204 mmol, 1 equiv.) was then added as a tetrahydrofuran solution resulting in an immediate color change

to a dark red. The solution was allowed to stir for 30 minutes before filtering the solution through a Celite pad. Tetrahydrofuran washes eluted further product from the Celite pad. The combined tetrahydrofuran filtrate was dried under reduced pressure to yield a red residue. This residue was recrystallized from acetonitrile:diethyl ether to yield the product as dark red crystals. Yield: 56.1 mg (31.6 %). *Note*: the product is not indefinitely stable in solution and eventually decomposes to a mixture of species. However, it is stable in the solid state. ^{1}H NMR (300 MHz, CD_3CN) δ 8.18 (broad s, O*H*, 2H), 7.86 (m, Ar*H*, 2H), 7.79 – 7.65 (m, Ar*H*, 4H), 7.59 (m', Ar*H*, 2H), 6.72 (s, central Ar*H*, 2H), 3.12 (m, C*H*, 4H), 1.42 – 1.07 (m, C*H*$_3$, 24H). ^{13}C{^{1}H} NMR (126 MHz, CD_3CN) δ 148.17 (s), 143.58 (s), 133.80 (s), 133.23 (s), 132.55 (s), 130.76 (s), 130.14 (s), 128.81 (s), 128.28 (s), 27.35 (s), 26.89 (vt, J_{PC} = 11.5 Hz), 19.61 (s), 19.34 (s), 18.74 (s). ^{31}P{^{1}H} NMR (121 MHz, CD_3CN) δ 34.22 (s). ^{19}F NMR (282 MHz, CD_3CN) δ -79.40 (s). Anal. Calcd. for: $C_{31}H_{44}F_3O_5P_2PdS$ (**5)** (%): C, 47.40; H, 4.51. Found: C, 47.62; H, 5.13.

Synthesis of Complex 6-H

Pyridinium triflate (44.7 mg, 0.195 mmol, 1 equiv.) was partially dissolved in tetrahydrofuran (4 mL) in a 20 mL scintillation vial. Compound **4-H** (117.2 mg, 0.195 mmol, 1 equiv.) was the added as a tetrahydrofuran solution which resulted in an immediate lightening of the solution from yellow/brown to yellow. After stirring for 16 hours the reaction mixture was dried under reduced pressure to yield the product as a foamy yellow/orange solid in quantitative yield. ^{1}H NMR (300 MHz, CD_3CN) δ 7.84 – 7.75 (m, Ar*H*, 2H), 7.71 – 7.53 (m, Ar*H*, 6H), 7.42 (broad s, O*H*, 2H), 6.79 (s, central Ar*H*, 4H), 2.46 (m, C*H*, 4H), 1.19 – 1.01 (m, C*H*$_3$, 18H), 0.94 (m, C*H*$_3$, 6H), -16.33 (t, J_{PH} = 8.5 Hz, Pd*H*, 1H). ^{13}C{^{1}H} NMR (126

MHz, CD_3CN) δ 144.58 (s), 143.99 (vt, J_{PC} = 7.2 Hz), 132.28 (s), 131.11 (s), 130.12 (s), 128.38 (s), 126.64 (s), 125.97 (vt, J_{PC} = 19.2 Hz), 110.30 (s), 28.11 (vt, J_{PC} = 13.1 Hz), 27.30 (vt, J_{PC} = 12.5 Hz), 19.68 (s), 19.44 (s), 18.60 (s), 18.41 (s). $^{31}P\{^1H\}$ NMR (121 MHz, CD_3CN) δ 41.57 (d, J_{PH} = 6.7 Hz). ^{19}F NMR (282 MHz, CD_3CN) δ -79.34 (s). Anal. Calcd. for: $C_{31}H_{41}F_3O_5P_2PdS$ (**6)** (%): C, 49.57; H, 5.50. Found: C, 49.32; H, 5.36.

Synthesis of Complex 7-H

Compound **1-H** (129.5 mg, 0.262 mmol, 1 equiv.) was dissolved in tetrahydrofuran (8 mL) and then added to a 20 mL scintillation vial with silver triflate (67.2 mg, 0.262 mmol, 1 equiv.). The reaction mixture was allowed to stir for 3 hours to yield a pale pink solution before being dried under reduced pressure. The residue was then dissolved in minimal acetonitrile and filtered through a Celite pad, which removed the pinkish color. The product was then recrystallized from an acetonitrile:diethyl ether vapor diffusion to yield white crystalline needles. Yield: 134 mg (68 %). ^1H NMR (500 MHz, CD_3CN) δ 7.81 – 7.77 (m, Ar*H*, 2H), 7.72 – 7.68 (t, J_{HH} = 7.6 Hz, 2H), 7.63 (t, J_{HH} = 7.7 Hz, Ar*H*, 2H), 7.58 (dq, J_{HH} = 7.5 Hz, J_{HH} = 1.8 Hz, Ar*H*, 2H), 6.98 (broad s, O*H*, 2H), 6.85 (s, central Ar*H*, 2H), 2.52 (m, C*H*, 4H), 1.32 – 1.15 (m, C*H*$_3$, 12H), 1.02 (m, C*H*$_3$, 12H). $^{13}C\{^1H\}$ NMR (126 MHz, CD_3CN) δ 147.80 (s), 144.47 (vt, J_{PC} = 8.7 Hz), 132.62 (d), 131.00 (s), 130.30 (s), 128.58 (s), 126.91 (d, J_{PC} = 5.3 Hz), 126.88 – 126.48 (m), 118.16 (s), 26.12 (dd), 25.78 – 25.34 (m), 20.93 (vt, J_{PC} = 5.9 Hz), 20.65 (vt, J_{PC} = 5.9 Hz), 19.50 (m). $^{31}P\{^1H\}$ NMR (121 MHz, CD_3CN) δ 28.33 (d, J_{PAg} = 559.7 Hz), 28.33 (d, J_{PAg} = 484.9 Hz). ^{19}F NMR (282 MHz, CD_3CN) δ -79.32 (s). Anal. Calcd. for: $C_{31}H_{40}AgF_3O_5P_2S$ (**7)** (%): C, 49.54; H, 5.37. Found: C, 49.77; H, 5.15.

Synthesis of Complex 4-Me

Compound **1-Me** (327.3 mg, 0.626 mmol, 1 equiv.) was dissolved in tetrahydrofuran (10 mL) and transferred to a Schlenk tube fitted with a screw-in Teflon stopper. (1,5-cyclooctadiene)palladium(II) dichloride was then added as a partially dissolved suspension in tetrahydrofuran (15 mL). The reaction mixture was allowed to stir for 2 hours during which time the solution became a homogeneous yellow/orange. (1,5-cyclooctadiene)(2,2'-bipyridine)nickel(0) was added as a solution in tetrahydrofuran (20 mL) which resulted in immediate consumption of the purple nickel complex and the formation of a heterogeneous orange solution. The reaction mixture was stirred for an additional 30 minutes before filtering through a Celite pad. Additional tetrahydrofuran was used to wash product through the Celite pad. The combined tetrahydrofuran filtrate was dried under reduced pressure to yield an orange residue. This residue was redissolved in benzene and lyophilized to yield the product as an orange powder. Yield: 385.8 mg (98 %). ^{1}H NMR (300 MHz, C_6D_6) δ 7.63 (m, Ar*H*, 2H), 7.45 (m, Ar*H*, 12H), 7.22 (m, Ar*H*, 4H), 6.86 (s, central Ar*H*, 2H), 3.49 (s, OC*H*$_3$, 6H), 1.96 (m, C*H*, 4H), 1.36 (m, C*H*$_3$, 12H), 1.00 (m, C*H*$_3$, 12H). ^{13}C{^{1}H} NMR (126 MHz, C_6D_6) δ 149.30 (s), 147.29 (vt, J_{PC} = 10.0 Hz), 133.88 (vt, J_{PC} = 10.9 Hz), 131.25 (s), 129.95 (s), 126.81 (s), 125.74 (s), 55.09 (s), 28.58 (vt, J_{PC} = 6.2 Hz), 28.40 (t, J_{PC} = 6.3 Hz), 22.18 (vt, J_{PC} = 8.6 Hz), 21.97 (vt, J_{PC} = 8.8 Hz), 20.82 (s), 20.52 (s). ^{31}P{^{1}H} NMR (121 MHz, C_6D_6) δ 33.81 (s). Anal. Calcd. for: $C_{32}H_{44}O_2P_2Pd$ (**9)** (%): C, 61.10; H, 7.05. Found: C, 60.62; H, 6.81.

Synthesis of Complex 6-Me

Pyridinium triflate (94.8 mg, 0.413 mmol, 1 equiv.) was partially dissolved in tetrahydrofuran (5 mL) in a 20 mL scintillation vial. Compound **4-Me** (260.3 mg, 0.413 mmol,

1 equiv.) was then added as a tetrahydrofuran solution (10 mL) which resulted in an immediate color change from orange to yellow. After stirring for 16 hours the reaction mixture was dried under reduced pressure to yield the product as a foamy yellow/orange solid in quantitative yield. ^{1}H NMR (300 MHz, CD_3CN) δ 7.86 – 7.75 (m, Ar*H*, 2H), 7.75 – 7.51 (m, Ar*H*, 6H), 6.99 (s, central Ar*H*, 2H), 3.73 (s, OC*H*$_3$, 1H), 2.55 – 2.42 (m, C*H*, 4H), 1.17 – 1.01 (m, C*H*$_3$, 12H), 1.00 – 0.84 (m, C*H*$_3$, 12H), -16.33 (t, J_{PH} = 9.0 Hz, Pd*H*, 1H).^{13}C{^{1}H} NMR (126 MHz, CD_3CN) δ 148.03 (s), 144.17 (vt, J_{PC} = 7.0 Hz), 132.17 (s), 130.98 (s), 128.39 (s), 127.92 (s), 125.55 (vt, J_{PC} = 19.0 Hz), 107.70 (s), 56.49 (d), 27.76 (vt, J_{PC} = 13.3 Hz), 27.18 (vt, J_{PC} = 13.2 Hz), 19.63 (s), 19.24 (s), 18.55 (s), 18.22 (s). ^{31}P{^{1}H} NMR (121 MHz, CD_3CN) δ 41.93 (s). ^{19}F NMR (282 MHz, CD_3CN) δ -79.37 (s). Anal. Calcd. for: $C_{33}H_{45}F_3O_5P_2PdS$ (**10)** (%): C, 50.87; H, 5.82. Found: C, 50.19; H, 5.47.

In Situ Preparation of Complex 8-Me

4-Me (11.6 mg, 0.0184 mmol, 1 equiv) was dissolved d_8-THF and transferred to a J-Young tube. The solution was then frozen and the headspace removed under vacuum. Excess O_2 (1 atm) was then added and the solution was carefully mixed to avoid warming the solution. Immediate and quantitative conversion to **8-Me** was observed by NMR at -78 °C. *Note:* The compound is stable at low temperatures with no decomposition detected by NMR for hours at -40 °C or two weeks at -78 °C. However, around 0 °C decomposition to a mixture of species in observed. Solutions can be degassed to remove excess O_2 by placing solutions under dynamic vacuum at -78 °C if prepared in a Schlenk tube or by multiple freeze-pump-thaw cycles if care is taken not to warm the solution above -40 °C. All NMR characterization was obtained at -40 °C. ^{1}H NMR (500 MHz, d_8-THF) δ 7.62 (dd, J_{HH} = 7.8 Hz, J_{HH} = 5.1 Hz, Ar*H*,

1H), 7.54 (dd, J_{HH} = 7.8, J_{HH} = 5.1 Hz, Ar*H*, 1H), 7.52 – 7.46 (m, Ar*H*, 4H), 7.44 – 7.38 (m, Ar*H*, 2H), 6.87 (s, central aryl Ar*H*, 1H), 6.66 (s, central aryl Ar*H*, 1H), 3.56 (s, OC*H*$_3$, 3H), 3.47 (s, OC*H*$_3$, 3H), 2.67 (m, C*H*, 1H), 2.59 (m, C*H*, 1H), 1.98 (m, C*H*, 2H), 1.37 (m, C*H*$_3$, 12H), 1.13 – 1.04 (m, C*H*$_3$, 6H), 0.85 (m, C*H*$_3$, 6H). $^{13}C\{^1H\}$ NMR (126 MHz, d_8-THF) δ 151.03 (s), 149.81 (s), 146.60 (d, J_{PC} = 16.0 Hz), 145.46 (d, J_{PC} = 16.1 Hz), 133.84 (s), 133.06 (s), 132.99 (s), 132.77 (s), 130.28 (s), 130.09 (s), 129.66 (d, J_{PC} = 6.1 Hz), 129.52 (d, J_{PC} = 5.8 Hz), 129.14 (s), 128.95 (d, J_{PC} = 7.2 Hz), 128.78 (s), 128.61 (d, J_{PC} = 6.6 Hz), 128.21 (s), 127.97 (s), 127.87 (s), 127.67 (s), 127.48 (s), 126.06 (s), 125.53 (s), 113.70 (d, J_{PC} = 13.2 Hz), 54.43 (s), 28.36 (d, J_{PC} = 14.2 Hz), 27.26 (d, J_{PC} = 11.5 Hz), 25.48 (d, J_{PC} = 20.2 Hz), 22.70 (d, J_{PC} = 18.0 Hz), 22.37 (d, J_{PC} = 15.1 Hz), 20.04 (s), 19.53 (d, J_{PC} = 13.1 Hz), 19.33 (d, J_{PC} = 7.1 Hz), 18.86 (d, J_{PC} = 5.6 Hz), 17.26 (d, J_{PC} = 4.5 Hz), 16.32 (d, J_{PC} = 6.0 Hz). $^{31}P\{^1H\}$ NMR (202 MHz, d_8-THF) δ 34.04 (d, $^2J_{PP}$ = 23.8 Hz), 29.87 (d, $^2J_{PP}$ = 24.0 Hz).

Synthesis of Complex (3)H$^+$

6-H (13.9 mg, 0.019 mmol, 1 equiv) was dissolved in CD_3CN and transferred to a J-Young tube. The solution was then frozen and the headspace removed under vacuum. Excess O_2 (1 atm) was then added and the sample was allowed to thaw to room temperature with inversion to ensure adequate mixing. A gradual color change from yellow/orange to a pink/red solution was observed over 6^+ hours. NMR revealed quantitative conversion to a new species, **(3)H$^+$**, that could be isolated as a red powder following removal of volatiles. ^1H NMR (300 MHz, CD_3CN) δ 7.76 – 7.51 (m, 8H), 6.39 (s, 2H), 2.63 (m, 2H), 2.54 (m, 2H), 1.24 – 0.96 (m, 24H). ^{13}C NMR (126 MHz, CD_3CN) δ 142.35 (d, J_{PC} = 13.7 Hz), 139.70 (d, J_{PC} = 37.2 Hz), 133.34 (s), 132.23 (s), 131.57 (s), 129.09 (d, J_{PC} = 13.6 Hz), 127.38 (s), 105.94 (s), 28.10 (d, J_{PC} = 19.1

Hz), 26.35 (d, J_{PC} = 26.1 Hz), 18.73 (s), 18.07 (s), 17.83 (s), 17.23 (s). ^{31}P NMR (121 MHz, CD_3CN) δ 64.39. ^{19}F NMR (282 MHz, CD_3CN) δ -79.34.

Volumetric Measurement of O_2 Consumption

Toepler Pump Experimental Details

To determine the stoichiometry of reaction of O_2 with compounds **4-**H, **4-Me**, and 6-H, a solution of the compound to be tested was degassed via three freeze-pump-thaw cycles on a high vacuum line. While the solution (benzene for **4-H**, THF for **4-Me** and **6-H**) was still frozen, a known amount of O_2 (~3-5 equiv) was measured with a volumetric Schlenk bulb (33.28 mL or 43.48 mL). The exact procedure then varied depending on the compound used. For **4-H** and **6-H**, the solution of compound was then warmed to room temperature and while stirring vigorously the O_2 was then added to the reaction mixture. For **4-Me**, the solution was warmed to -78 °C and while stirring vigorously the dioxygen was added to the reaction mixture while this temperature was maintained. All reactions were allowed to stir for 1hr. During this time, the solution of **4-H** and **6-H** were observed to change color from brown/yellow and pale yellow to purple and pink respectively. No substantial color changed was observed following O_2 addition to **4-Me** at low temperature. The solution was again frozen, and the gas present in the headspace was measured by Toepler pump (30.23 mL volume). Three freeze-pump-thaw cycles were carried out on the final reaction solution to recover all unreacted gases. Table **1** summarizes all the separate runs of volumetric measurements.

Table 1. Results of volumetric O_2 measurements. Volumetric bulb volume = 33.28 mL[a] or 43.48 mL[b], Toepler pump volume = 30.25 mL.

Run	Cmpd	T (K)	mmol Cmpd	O_2 added (mmHg)	Final O_2 (mmHg)	mmol O_2 Consumed	Equiv Consumed
1[a]	**4-H**	295	0.0902	151	197	0.0507	0.56
2[a]	**4-H**	295	0.0928	152	197	0.0490	0.53
3[b]	**4-H**	295	0.0850	182	234	0.0454	0.53
4[b]	**6-H**	295	0.0808	186	224	0.0712	0.88
5[b]	**6-H**	295	0.0800	190	227	0.0758	0.95
6[b]	**6-H**	295	0.0750	187	226	0.0703	0.94
7[b]	**4-Me**	295	0.0849	157	172	0.0882	1.04
8[b]	**4-Me**	295	0.0885	157	178	0.0783	0.89
9[b]	**4-Me**	295	0.0909	159	176	0.0863	0.95

ReactIR Spectra

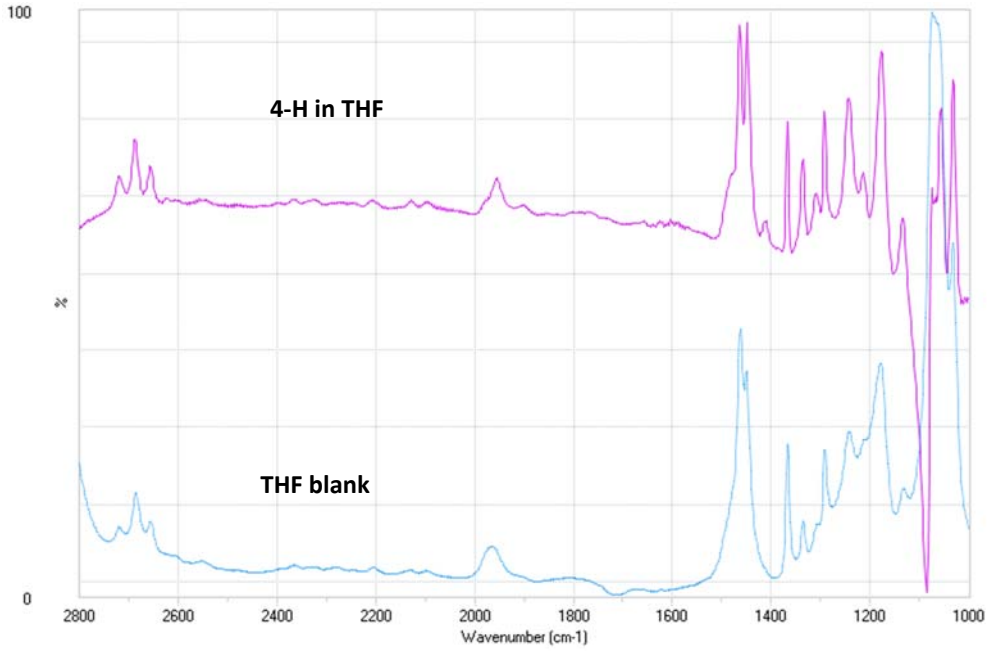

Figure 16. Solution ReactIR spectrum for **4-H** at -78 °C before O_2 addition.

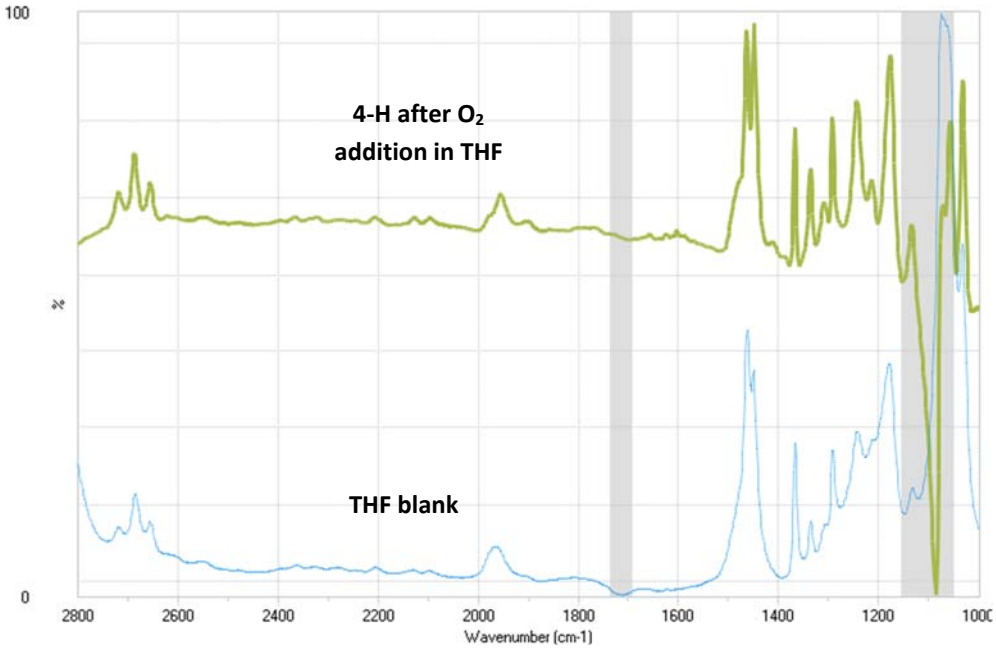

Figure 17. Solution ReactIR spectrum for **4-H** at -78 °C after O_2 addition.

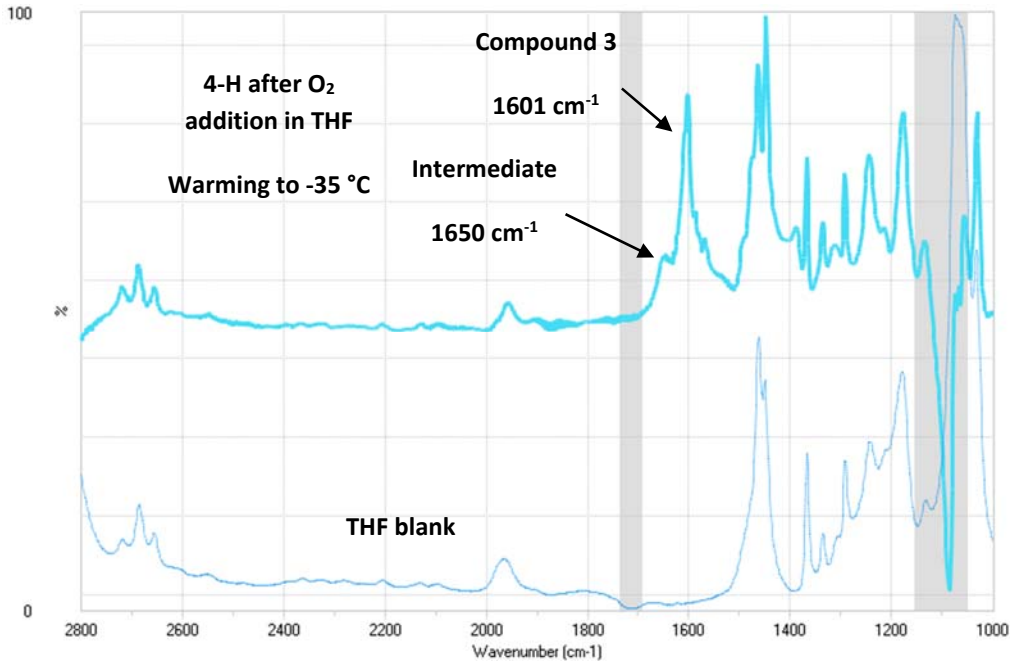

Figure 18. Solution ReactIR spectrum for **4-H** after warming to -35 °C after O_2 addition.

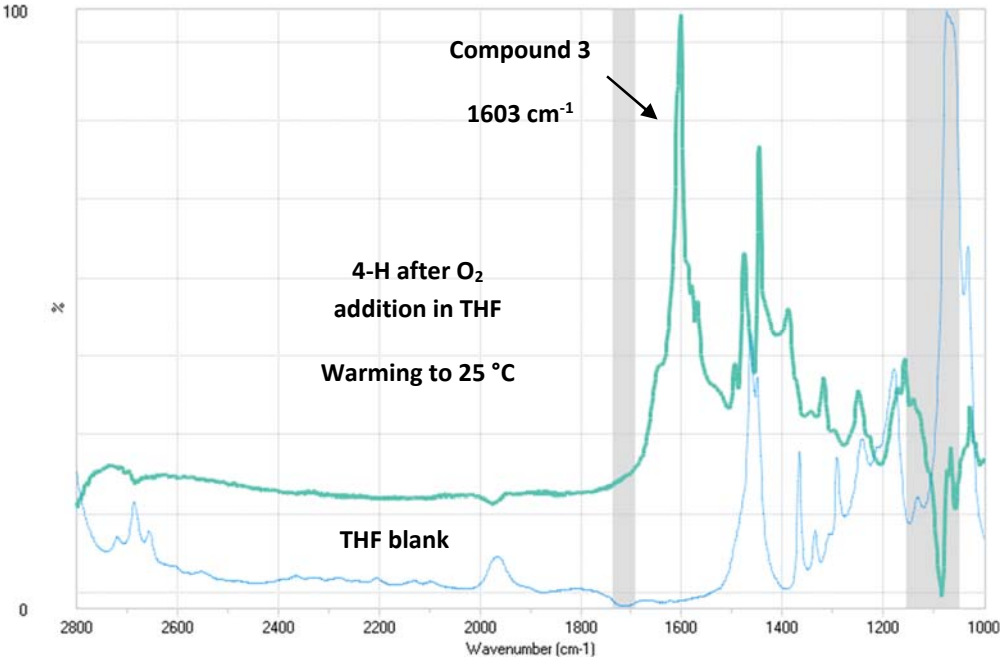

Figure 19. Solution ReactIR spectrum for **4-H** after warming to 25 °C after O_2 addition.

UV/Vis Spectra

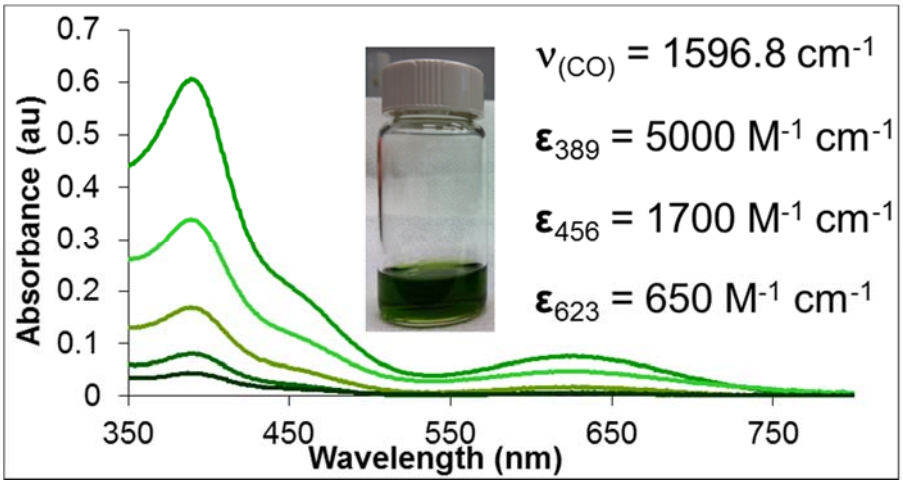

Figure 20. Solution UV/Vis spectrum for **2**.

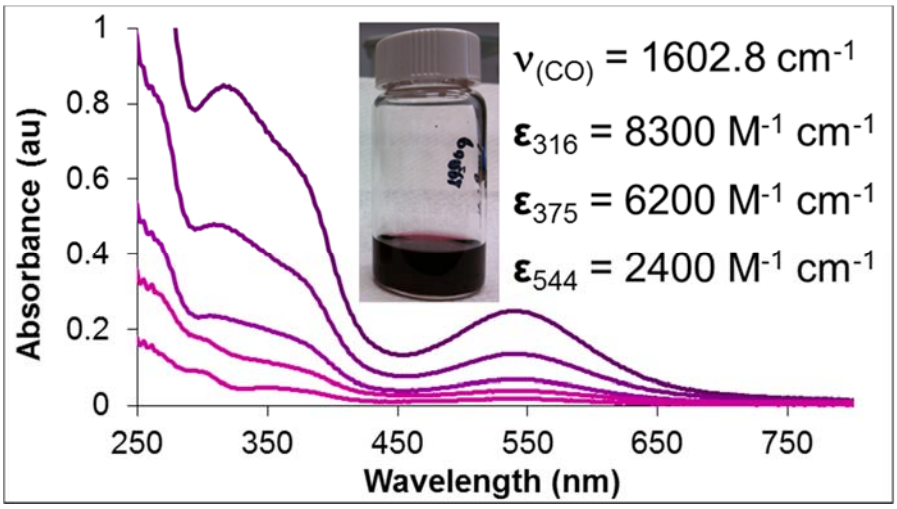

Figure 21. Solution UV/Vis spectrum for **3**.

Oxidation of 4-H to 3 by Various Substrates

Dioxygen

4-H (10.1 mg, 0.0170 mmol, 1 equiv) was transferred to a Schlenk tube as a solution in ca. 2 mL of THF. The solution was degassed by three freeze-pump-thaw cycles and then cooled to -78 °C. Excess O_2 (1 atm) was then added and allowed to stir vigorously for several minutes. The reaction mixture was then degassed under dynamic vacuum at -78 °C while stirring vigorously for 8 minutes. The reaction mixture was then warmed to room temperature. During this time the solution immediately turned purple indicative of the formation of **3**. Volatiles were then removed under reduced pressure and NMR of the residue taken in C_6D_6, which confirmed the quantitative formation of **3**. If the reaction is run in a J-Young tube in C_6D_6 the formation of water could be confirmed by vacuum transferring the volatiles of the reaction into another J-Young tube.

Nitric Oxide

4-H (10.0 mg, 0.0167 mmol, 1 equiv) was dissolved in C_6D_6 and transferred to a J-Young tube. The sample was frozen and the headspace removed. Nitric oxide (1 equiv) was measured in a calibrated gas bulb and then condensed into the J-Young tube. The sample was then warmed to room temperature. The solution turned purple as soon it thawed indicating the rapid formation of **3**. This was confirmed by NMR which showed quantitative conversion to **3**. The formation of water could be confirmed by vacuum transferring the volatiles of the reaction into another J-Young tube.

Nitrous Oxide

4-H (9.9 mg, 0.0165 mmol, 1 equiv) was dissolved in C_6D_6 and transferred to a J-Young tube. The sample was frozen and the headspace removed. Excess nitrous oxide (1 atm) was then added to the J-Young tube. The sample was then warmed to room temperature. The reaction was then monitored by NMR. The slow formation of **3** was observed by NMR over the course of 12 hrs, however simultaneous decomposition of **4-H** typical of solution samples allowed to stand has also occurred. A color change from brown-yellow to a purple was observed over the course of the reaction. The formation of water could be confirmed by vacuum transferring the volatiles of the reaction into another J-Young tube.

2,4,6-Tri(tertbutyl) Phenoxyl Radical

4-H (10.0 mg, 0.0167 mmol, 1 equiv) was dissolved in ca. 1 mL of THF and transferred to a 20 mL scintillation vial equipped with a magnetic stirbar. 2,4,6-tri*tert*butyl phenoxyl radical (8.2 mg, 0.033 mmol, 2 equiv) as then added as a solution in ca. 1 mL THF. This resulted in the immediate formation of a purple solution consistent with formation of **3**. The volatiles were then removed under reduced pressure. Successful conversion to **3** was confirmed by ^{31}P NMR.

1-Azido Adamantane

4-H (10.6 mg, 0.0180 mmol, 1 equiv) was dissolved in ca. 1 mL of THF and transferred to a 20 mL scintillation vial equipped with a magnetic stirbar. 1-Azido adamantane (3.2 mg,

0.0180 mmol, 1 equiv) was added as a solution in ca. 1 mL of THF and the reaction was allowed to stir for 2 hrs. During this time the solution turned from yellow-brown to purple, indicative of conversion to **3**. The volatiles were then removed under reduced pressure. Successful conversion to **3** was confirmed by ^{31}P NMR. The formation of 1-amino adamantine was confirmed by GC-MS comparisons to the retention time and mass data for an authentic sample.

Trimethylamine n-oxide

4-H (10.0 mg, 0.0166 mmol, 1 equiv) was dissolved in ca. 1 mL of MeCN and transferred to a 20 mL scintillation vial equipped with a magnetic stirbar. Trimethylamine *n*-oxide (1.3 mg, 0.0173 mmol, 1.04 equiv) was added as a solution in ca. 1 mL of MeCN and the reaction was allowed to stir for 2 hrs. During this time the solution turned from yellow-brown to purple, indicative of conversion to **3**. The volatiles were then removed under reduced pressure. Successful conversion to **3** was confirmed by ^{31}P NMR.

1,4-Benzoquinone

4-H (10.0 mg, 0.0166 mmol, 1 equiv) was dissolved in ca. 1 mL of THF and transferred to a 20 mL scintillation vial equipped with a magnetic stirbar. 1,4-Benzoquinone (1.8 mg, 0.167 mmol, 1 equiv) was then added as a solution in ca. 1 mL of THF and the reaction was allowed to stir for 2 hrs. During this time there was a rapid color change from brown-yellow to purple, indicative of conversion to **3**. The volatiles were then removed under reduced pressure. Successful conversion to **3** was confirmed by ^{31}P NMR.

Representative Conditions for Testing Substrate Oxidation by 8-Me

Para-trifluoromethyl benzyl alcohol

In a Schlenk tube equipped with a magnetic stirbar, **4-Me** (11.3 mg, 0.0180 mmol, 1 equiv) and 1,3,5-trimethoxybenzene (3.7 mg, 0.0180 mmol, 1 equiv), for an internal standard, was dissolved in ca. 5 mL of THF. The solution was degassed by a series of three freeze-pump-thaw cycles, then cooled to -78 °C. Excess O_2 (1 atm) was then added the solution was stirred vigorously to ensure complete conversion to **8-Me** The solution was then degassed under dynamic vacuum at -78 °C while stirring vigorously for several minutes. The reaction was then put under a N_2 atmosphere and para-trifluoromethyl benzyl alcohol (24.6 μL, 0.180 mmol, 10 equiv) was added via syringe. The reaction mixture was allowed to stir for 4 hrs before a GC-MS aliquot was taken under a strong counterflow of N_2. GC-MS indicated partial conversion to the corresponding benzaldehyde and unreacted benzyl alcohol by comparison to retention time and mass data for authentic samples. Addition of more equivalents of O_2 did not lead to further conversion to product.

Para-trifluoromethyl-benzaldehyde

No oxidation of the benzaldehyde was observed by GC-MS.

Cyclohexane Carboxaldehyde

Partial conversion to cyclohexene observed by GC by comparison to retention time for an authentic sample.

Cyclohexene

No oxidation of cyclohexene was observed by GC. In particular, no cyclohexanone was observed by comparison to retention time for an authentic sample.

Triphenylphosphine

Partial conversion to triphenylphosphine oxide observed by GC-MS by comparison to retention time and MS data for an authentic sample. However, low temperature ^{31}P NMR experiments indicate that substitution of **1-Me** by 2 equivalents of PPh_3 to yield $(PPh_3)_2Pd(\eta^2\text{-}O_2)$ occurs (^{31}P shift observed at 33.18 ppm consistent with literature data obtained in DMF (33.4 ppm) or $CDCl_3$ (33.2 ppm)). By comparison to the ^{31}P integration of against an internal standard of $OP(OMe)_3$, the disappearance of **8-Me** occurs at the same rate of **1-Me** and $(PPh_3)_2Pd(\eta^2\text{-}O_2)$ formation. Subsequent formation of phosphine oxide observed by GC-MS likely occurs from this complex rather than **8-Me**.

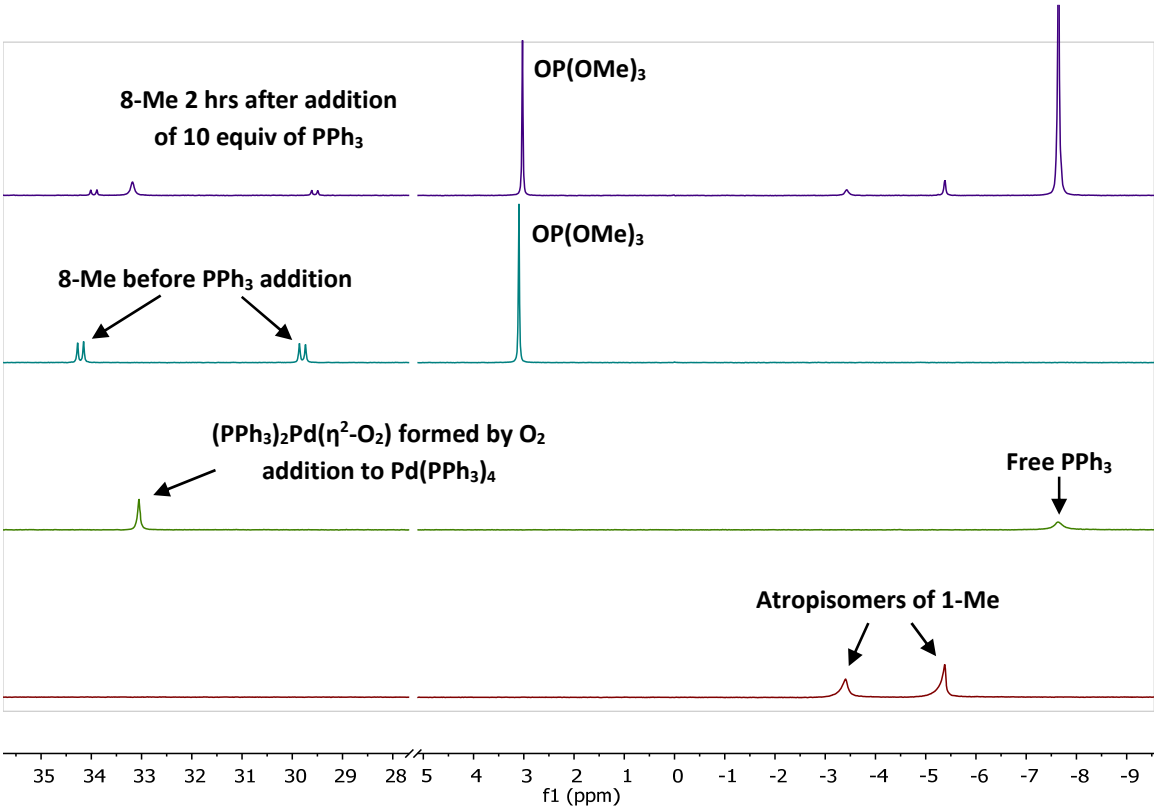

Figure 22. NMR spectra taken at -78 °C in THF confirming the substitution of PPh_3 for **1-Me** in solution in compound **8-Me**.

Methyl-para-tolyl sulfide

No oxidation of the aryl-alkyl sulfide was observed.

Electrochemical Details

Electrochemical measurements of complex **2** and **3** were taken on a Pine Instrument Company biopotentiostat model AFCBP1 as 3 millimolar solutions in tetrahydrofuran using 0.1 molar [*n*Bu_4N][PF_6] as the electrolyte with a platinum wire counter electrode, a glassy carbon working electrode, and a silver/silver nitrate reference electrode in 0.1 molar [*n*Bu_4N][PF_6] as an acetonitrile solution. Electrochemical measurements of compounds were internally referenced to ferrocene.

Crystallographic Information

CCDC 1440560-1440565 contain the supplementary crystallographic data for this paper. These data can be obtained free of charge from The Cambridge Crystallographic Data Centre via www.ccdc.cam.ac.uk/data_request/cif.

Refinement details

In each case, crystals were mounted on a glass fiber or nylon loop using Paratone oil, then placed on the diffractometer under a nitrogen stream. Low temperature (100 K) X-ray data were obtained on a Bruker APEXII CCD based diffractometer (Mo sealed X-ray tube, K_α = 0.71073 Å). All diffractometer manipulations, including data collection, integration and scaling were carried out using the Bruker APEXII software.[35] Absorption corrections were applied using SADABS.[36] Space groups were determined on the basis of systematic absences and intensity statistics and the structures were solved by direct methods using XS (incorporated into SHELXTL) and refined by full-matrix least squares on F^2. All non-hydrogen atoms were refined using anisotropic displacement parameters. Hydrogen atoms were placed in idealized positions and refined using a riding model. The structure was refined (weighted least squares refinement on F^2) to convergence.

Table 2. Crystal and refinement data for reported complexes.

Complex	**2**	**3**	**4-H**	**5-H**	**6-H**	**7-H**
empirical formula	$C_{15}H_{19}Cl_{0.06}Ni_{0.50}OP$	$C_{32}H_{43}O_{2.5}P_2Pd$	$C_{69}H_{88}O_4P_4Pd_2$	$C_{35}H_{48}F_3ClO_6P_2PdS$	$C_{31}H_{41}F_3O_5P_2PdS$	$C_{32.33}H_{43.33}AgF_3O_{5.33}P_2S$
formula wt	277.84	636.00	1318.07	857.58	751.04	776.20
T (K)	100	200	100	100	100	99.98
a, Å	16.8334(5)	24.0630(6)	12.900(3)	13.040(6)	19.7535(3)	31.152(3)
b, Å	16.8334(5)	24.0630(6)	13.564(3)	19.284(8)	19.7535(3)	31.152(3)
c, Å	20.9194(8)	20.9789(6)	19.638(3)	15.679(6)	19.7535(3)	20.2695(18)
α, deg	90	90	106.655(6)	90	110.8200	90
β, deg	90	90	91.342(6)	108.373(18)	110.8200	90
γ, deg	90	90	97.356(5)	90	110.8200	120
V, Å^3	5927.8(4)	12147.4(7)	3258.4(12)	3742(3)	5617.9(3)	17035
Z	16	16	4	4	6	18
cryst syst	Tetragonal	Tetragonal	Triclinic	Monoclinic	Rhombohedral	Trigonal
space group	P2/ncc	P-42$_1$c	P-1	P12$_1$/n1	R3cR	R3c
d_{calcd}, g/cm^3	1.245	1.391	1.344	1.515	1.332	1.362
θ range, deg	1.711 to 36.343	1.197 to 37.310	1.583 to 37.026	1.729 to 36.211	2.17 to 29.22	2.147 to 30.664
μ, mm^{-1}	0.797	0.745	0.696	0.767	0.685	0.723
abs cor	Semi-empirical from equivalents	Semi-empirical from equivalents	Semi-empirical from equivalents	Semi-empirical from equivalents	Semi-empirical from equivalents	Semi-empirical from equivalents
GOF[c]	0.952	1.167	0.874	1.022	0.972	0.904
R1,[a] wR2[b] ($I > 2\sigma(I)$)	0.0406, 0.1039	0.0527, 0.0995	0.0521, 0.0944	0.0529, 0.1286	0.0318, 0.0720	0.0475, 0.1239

[a] $R1 = \Sigma||F_o|-|F_c|| / \Sigma|F_o|$ [b] $wR2 = \{ \Sigma [w(F_o^2-F_c^2)^2] / \Sigma [w(F_o^2)^2] \}^{1/2}$ [c] $GOF = S = \{ \Sigma [w(F_o^2-F_c^2)^2] / (n-p) \}^{1/2}$

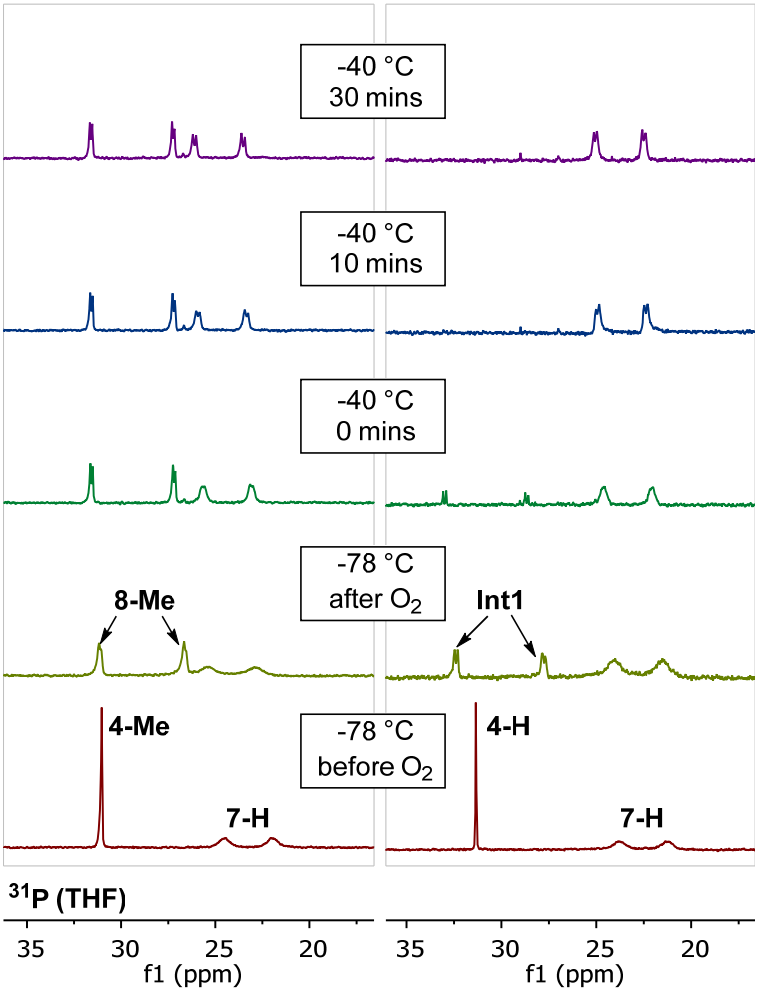

Figure 23. NMR spectra taken at -78 °C in THF confirming the substitution of PPh_3 for **1-Me** in solution in compound **8-Me**.

REFERENCES

1.(a) Costas, M.; Mehn, M. P.; Jensen, M. P.; Que, L., *Chem. Rev.* **2004,** *104*, 939-986; (b) Sono, M.; Roach, M. P.; Coulter, E. D.; Dawson, J. H., *Chem. Rev.* **1996,** *96*, 2841-2888; (c) Whittaker, J. W., *Chem. Rev.* **2003,** *103*, 2347-2363.

2.(a) Chirik, P. J.; Wieghardt, K., *Science* **2010,** *327*, 794-795; (b) Eisenberg, R.; Gray, H. B., *Inorg. Chem.* **2011,** *50*, 9741-9751; (c) Haneline, M. R.; Heyduk, A. F., *J. Am. Chem. Soc.* **2006,** *128*, 8410-8411; (d) Luca, O. R.; Crabtree, R. H., *Chem. Soc. Rev.* **2013,** *42*, 1440-1459; (e) Lyaskovskyy, V.; de Bruin, B., *ACS Catal.* **2012,** *2*, 270-279; (f) Pierpont, C. G., *Coord. Chem. Rev.* **2001,** *216–217*, 99-125; (g) Praneeth, V. K. K.; Ringenberg, M. R.; Ward, T. R., *Angew. Chem. Int. Ed.* **2012,** *51*, 10228-10234; (h) Brown, S. N., *Inorg. Chem.* **2012,** *51*, 1251-1260.

3.(a) Chang, C. J.; Chng, L. L.; Nocera, D. G., *J. Am. Chem. Soc.* **2003,** *125*, 1866-1876; (b) Chaudhuri, P.; Hess, M.; Müller, J.; Hildenbrand, K.; Bill, E.; Weyhermüller, T.; Wieghardt, K., *J. Am. Chem. Soc.* **1999,** *121*, 9599-9610; (c) Hull, J. F.; Himeda, Y.; Wang, W.-H.; Hashiguchi, B.; Periana, R.; Szalda, D. J.; Muckerman, J. T.; Fujita, E., *Nat. Chem.* **2012,** *4*, 383-388; (d) Langer, R.; Leitus, G.; Ben-David, Y.; Milstein, D., *Angew. Chem. Int. Ed.* **2011,** *50*, 2120-2124; (e) Umehara, K.; Kuwata, S.; Ikariya, T., *J. Am. Chem. Soc.* **2013,** *135*, 6754-6757; (f) Vogt, M.; Nerush, A.; Diskin-Posner, Y.; Ben-David, Y.; Milstein, D., *Chem. Sci.* **2014,** *5*, 2043-2051; (g) Carver, C. T.; Matson, B. D.; Mayer, J. M., *J. Am. Chem. Soc.* **2012,** *134*, 5444-5447; (h) Gunanathan, C.; Milstein, D., *Acc. Chem. Res.* **2011,** *44*, 588-602; (i) Kohl, S. W.; Weiner, L.; Schwartsburd, L.; Konstantinovski, L.; Shimon, L. J. W.; Ben-David, Y.; Iron, M. A.; Milstein, D., *Science* **2009,** *324*, 74-77; (j) Rakowski DuBois, M.; DuBois, D. L., *Chem. Soc. Rev.* **2009,** *38*, 62-72.

4.(a) Costentin, C.; Drouet, S.; Robert, M.; Savéant, J.-M., *Science* **2012,** *338*, 90-94; (b) Purse, B. W.; Tran, L.-H.; Piera, J.; Åkermark, B.; Bäckvall, J.-E., *Chem. Eur. J.* **2008,** *14*, 7500-7503; (c) Warren, J. J.; Tronic, T. A.; Mayer, J. M., *Chem. Rev.* **2010,** *110*, 6961-7001; (d) McSkimming, A.; Colbran, S. B., *Chem. Soc. Rev.* **2013,** *42*, 5439-5488; (e) Collman, J. P.; Devaraj, N. K.; Decreau, R. A.; Yang, Y.; Yan, Y. L.; Ebina, W.; Eberspacher, T. A.; Chidsey, C. E. D., *Science* **2007,** *315*, 1565-1568; (f) Lu, F.; Zarkesh, R. A.; Heyduk, A. F., *Eur. J. Inorg. Chem.* **2012**, 467-470.

5.(a) Campbell, A. N.; White, P. B.; Guzei, I. A.; Stahl, S. S., *J. Am. Chem. Soc.* **2010,** *132*, 15116-15119; (b) Gligorich, K. M.; Sigman, M. S., *Chem. Commun.* **2009**, 3854-3867; (c) Muzart, J., *Chem. Asian J.* **2006,** *1*, 508-515; (d) Schultz, M. J.; Sigman, M. S., *Tetrahedron* **2006,** *62*, 8227-8241; (e) Shi, Z. Z.; Zhang, C.; Tang, C. H.; Jiao, N., *Chem. Soc. Rev.* **2012,** *41*, 3381-3430; (f) Sigman, M. S.; Jensen, D. R., *Acc. Chem. Res.* **2006,** *39*, 221-229; (g) Stahl, S. S., *Science* **2005,** *309*, 1824-1826; (h) Stoltz, B. M., *Chem. Lett.* **2004,** *33*, 362-367; (i) Piera, J.; Backvall, J. E., *Angew. Chem. Int. Ed.* **2008,** *47*, 3506-3523.

6.(a) Decharin, N.; Stahl, S. S., *J. Am. Chem. Soc.* **2011,** *133*, 5732-5735; (b) Diao, T.; Stahl, S. S., *Polyhedron* **2014,** *84*, 96-102; (c) Popp, B. V.; Thorman, J. L.; Stahl, S. S., *J. Mol. Cat.* **2006,** *251*, 2-7.

7.Wendlandt, A. E.; Stahl, S. S., *Angew. Chem. Int. Ed.* **2015,** *54*, 14638-14658.

8.Popp, B. V.; Stahl, S. S., *J. Am. Chem. Soc.* **2007,** *129*, 4410-4422.

9.(a) Kumar, A.; Purkait, K.; Dey, S. K.; Sarkar, A.; Mukherjee, A., *Rsc Adv* **2014,** *4*, 35233-35237; (b) Scheuermann, S.; Kretz, T.; Vitze, H.; Bats, J. W.; Bolte, M.; Lerner, H. W.; Wagner, M., *Chem. Eur. J.* **2008,** *14*, 2590-2601; (c) Sembiring, S. B.; Colbran, S. B.; Bishop, R.; Craig, D. C.; Rae, A. D., *Inorg. Chim. Acta* **1995,** *228*, 109-117; (d) Sembiring, S. B.; Colbran, S. B.; Craig, D. C., *Inorg. Chem.* **1995,** *34*, 761-762; (e) Sembiring, S. B.; Colbran, S. B.; Craig, D. C., *J. Chem. Soc., Dalton Trans.* **1999**, 1543-1554.

10.(a) Kim, S. B.; Pike, R. D.; Sweigart, D. A., *Acc. Chem. Res.* **2013,** *46*, 2485-2497; (b) Moussa, J.; Amouri, H., *Angew. Chem. Int. Ed.* **2008,** *47*, 1372-1380; (c) Reingold, J. A.; Uk Son, S.; Bok Kim, S.; Dullaghan, C. A.; Oh, M.; Frake, P. C.; Carpenter, G. B.; Sweigart, D. A., *Dalton Trans.* **2006**, 2385-2398; (d) Damas, A.; Ventura, B.; Axet, M. R.; Degli Esposti, A.; Chamoreau, L. M.; Barbieri, A.; Amouri, H., *Inorg. Chem.* **2010,** *49*, 10762-10764; (e) Le Bras, J.; Amouri, H.; Vaissermann, J., *Organometallics* **1998,** *17*, 1116-1121; (f) Moussa, J.; Rager, M. N.; Chamoreau, L. M.; Ricard, L.; Amouri, H., *Organometallics* **2009,** *28*, 397-404.
11.(a) Buss, J. A.; Edouard, G. A.; Cheng, C.; Shi, J.; Agapie, T., *J. Am. Chem. Soc.* **2014,** *136*, 11272-11275; (b) Chao, S. T.; Lara, N. C.; Lin, S.; Day, M. W.; Agapie, T., *Angew. Chem. Int. Ed.* **2011,** *50*, 7529-7532; (c) Henthorn, J. T.; Lin, S. B.; Agapie, T., *J. Am. Chem. Soc.* **2015,** *137*, 1458-1464; (d) Herbert, D. E.; Lara, N. C.; Agapie, T., *Chem. Eur. J.* **2013,** *19*, 16453-16460; (e) Horak, K. T.; Velian, A.; Day, M. W.; Agapie, T., *Chem. Commun.* **2014,** *50*, 4427-4429; (f) Kelley, P.; Lin, S.; Edouard, G.; Day, M. W.; Agapie, T., *J. Am. Chem. Soc.* **2012,** *134*, 5480-5483; (g) Lin, S.; Day, M. W.; Agapie, T., *J. Am. Chem. Soc.* **2011,** *133*, 3828-3831; (h) Suseno, S.; Agapie, T., *Organometallics* **2013,** *32*, 3161-3164; (i) Suseno, S.; Horak, K. T.; Day, M. W.; Agapie, T., *Organometallics* **2013,** *32*, 6883-6886; (j) Velian, A.; Lin, S.; Miller, A. J. M.; Day, M. W.; Agapie, T., *J. Am. Chem. Soc.* **2010,** *132*, 6296-6297.
12.Moore, H. W.; Sing, Y.-L. L.; Sidhu, R. S., *J. Org. Chem.* **1980,** *45*, 5057-5064.
13.(a) Glick, M. D.; Dahl, L. F., *J. Organomet. Chem.* **1965,** *3*, 200-&; (b) Klein, H. F.; Auer, E.; Dal, A.; Lemke, U.; Lemke, M.; Jung, T.; Rohr, C.; Florke, U.; Haupt, H. J., *Inorg. Chim. Acta* **1999,** *287*, 167-172; (c) Canovese, L.; Visentin, F.; Santo, C.; Bertolasi, V., *J. Organomet. Chem.* **2014,** *749*, 379-386; (d) Milani, B.; Anzilutti, A.; Vicentini, L.; Santi, A. S. O.; Zangrando, E.; Geremia, S.; Mestroni, G., *Organometallics* **1997,** *16*, 5064-5075; (e) Tschoerner, M.; Trabesinger, G.; Albinati, A.; Pregosin, P. S., *Organometallics* **1997,** *16*, 3447-3453.
14.(a) Schrauzer, G. N.; Dewhirst, K. C., *J. Am. Chem. Soc.* **1964,** *86*, 3265-3270; (b) Schrauzer, G. N.; Kratel, G., *J. Organomet. Chem.* **1964,** *2*, 336-346.
15.(a) Aleksand.Gg; Struchko.Yt, *Zh. Strukt. Khim.* **1973,** *14*, 1067-1074; (b) Yamamoto, Y.; Ohno, T.; Itoh, K., *Organometallics* **2003,** *22*, 2267-2272; (c) Selvakumar, K.; Zapf, A.; Spannenberg, A.; Beller, M., *Chem. Eur. J.* **2002,** *8*, 3901-3906.
16.(a) Clegg, W.; Eastham, G. R.; Elsegood, M. R. J.; Heaton, B. T.; Iggo, J. A.; Tooze, R. P.; Whyman, R.; Zacchini, S., *J. Chem. Soc., Dalton Trans.* **2002**, 3300-3308; (b) Kulik, A. V.; Bruk, L. G.; Temkin, O. N.; Khabibulin, V. R.; Belsky, V. K.; Zavodnik, V. E., *Mendeleev Commun.* **2002**, 47-48; (c) Liu, J. K.; Jacob, C.; Sheridan, K. J.; Al-Mosule, F.; Heaton, B. T.; Iggo, J. A.; Matthews, M.; Pelletier, J.; Whyman, R.; Bickley, J. F.; Steiner, A., *Dalton Trans.* **2010,** *39*, 7921-7935.
17.Kaftory, M.; Tanaka, K.; Toda, F., *J. Org. Chem.* **1985,** *50*, 2154-2158.
18.(a) Scheuermann, M. L.; Goldberg, K. I., *Chem. Eur. J.* **2014,** *20*, 14556-14568; (b) Boisvert, L.; Goldberg, K. I., *Acc. Chem. Res.* **2012,** *45*, 899-910.
19.(a) Aboelella, N. W.; York, J. T.; Reynolds, A. M.; Fujita, K.; Kinsinger, C. R.; Cramer, C. J.; Riordan, C. G.; Tolman, W. B., *Chem. Commun.* **2004**, 1716-1717; (b) Adjabeng, G.; Brenstrum, T.; Frampton, C. S.; Robertson, A. J.; Hillhouse, J.; McNulty, J.; Capretta, A., *J. Org. Chem.* **2004,** *69*, 5082-5086; (c) Erhardt, S.; Grushin, V. V.; Kilpatrick, A. H.; Macgregor, S. A.; Marshall, W. J.; Roe, D. C., *J. Am. Chem. Soc.* **2008,** *130*, 4828-4845; (d) Fantasia, S.; Egbert, J. D.; Jurcik, V.; Cazin, C. S. J.; Jacobsen, H.; Cavallo, L.; Heinekey, D. M.; Nolan, S. P., *Angew. Chem. Int. Ed.* **2009,** *48*, 5182-5186; (e) Fantasia, S.; Nolan, S. P., *Chem. Eur. J.* **2008,** *14*, 6987-6993; (f) Gramage-Doria, R.; Armspach, D.; Matt, D.; Toupet, L., *Chem. Eur. J.* **2012,** *18*, 10813-10816; (g) Halligudi, S. B.; Bhatt, K. N.; Khan, N. H.; Kurashy, R. I.; Venkatsubramanian, K., *Polyhedron* **1996,** *15*, 2093-2101; (h) Jurcik, V.; Schmid, T. E.;

Dumont, Q.; Slawin, A. M. Z.; Cazin, C. S. J., *Dalton Trans.* **2012,** *41*, 12619-12623; (i) Konnick, M. M.; Guzei, I. A.; Stahl, S. S., *J. Am. Chem. Soc.* **2004,** *126*, 10212-10213; (j) Labios, L. A.; Millard, M. D.; Rheingold, A. L.; Figueroa, J. S., *J. Am. Chem. Soc.* **2009,** *131*, 11318-11319; (k) Miyaji, T.; Kujime, M.; Hikichi, S.; Moro-oka, Y.; Akita, M., *Inorg. Chem.* **2002,** *41*, 5286-5295; (l) Sergeev, A. G.; Neumann, H.; Spannenberg, A.; Beller, M., *Organometallics* **2010,** *29*, 3368-3373; (m) Stahl, S. S.; Thorman, J. L.; Nelson, R. C.; Kozee, M. A., *J. Am. Chem. Soc.* **2001,** *123*, 7188-7189; (n) Tsubomura, T.; Murota, H.; Takao, K., *Inorg. Chem. Commun.* **2013,** *35*, 110-112; (o) Walther, D.; Lamm, K.; Gorls, H., *Z. Anorg. Allg. Chem.* **2009,** *635*, 1187-1195; (p) Yamashita, M.; Goto, K.; Kawashima, T., *J. Am. Chem. Soc.* **2005,** *127*, 7294-7295; (q) Yoshida, T.; Tatsumi, K.; Matsumoto, M.; Nakatsu, K.; Nakamura, A.; Fueno, T.; Otsuka, S., *Nouv. J. Chim.* **1979,** *3*, 761-774.
20.Cai, X. C.; Majumdar, S.; Fortman, G. C.; Cazin, C. S. J.; Slawin, A. M. Z.; Lhermitte, C.; Prabhakar, R.; Germain, M. E.; Palluccio, T.; Nolan, S. P.; Rybak-Akimova, E. V.; Temprado, M.; Captain, B.; Hoff, C. D., *J. Am. Chem. Soc.* **2011,** *133*, 1290-1293.
21.Scheuermann, M. L.; Boyce, D. W.; Grice, K. A.; Kaminsky, W.; Stoll, S.; Tolman, W. B.; Swang, O.; Goldberg, K. I., *Angew. Chem. Int. Ed.* **2014,** *53*, 6492-6495.
22.(a) Denney, M. C.; Smythe, N. A.; Cetto, K. L.; Kemp, R. A.; Goldberg, K. I., *J. Am. Chem. Soc.* **2006,** *128*, 2508-2509; (b) Keith, J. M.; Muller, R. P.; Kemp, R. A.; Goldberg, K. I.; Goddard, W. A.; Oxgaard, J., *Inorg. Chem.* **2006,** *45*, 9631-9633; (c) Konnick, M. M.; Decharin, N.; Popp, B. V.; Stahl, S. S., *Chem. Sci.* **2011,** *2*, 326-330; (d) Konnick, M. M.; Gandhi, B. A.; Guzei, I. A.; Stahl, S. S., *Angew. Chem. Int. Ed.* **2006,** *45*, 2904-2907.
23.(a) Goor, G.; Glenneberg, J.; Jacobi, S., Hydrogen Peroxide. In *Ullmann's Encyclopedia of Industrial Chemistry*, Wiley-VCH Verlag GmbH & Co. KGaA: 2000; (b) Nishimi, T.; Kamachi, T.; Kato, K.; Kato, T.; Yoshizawa, K., *Eur. J. Org. Chem.* **2011,** *2011*, 4113-4120.
24.Resonance Raman experiments in 2-methyl tetrahydrofuran using wavelengths accessible to an Ar ion laser were attempted for Int1 and 8-Me. Depending on the excitation wavelength no signals from compound were detected of fluorescence from the ligand precluded the observation of bands corresponding to the O-O stretch in the peroxo species.
25.(a) Geiger, R. A.; Chattopadhyay, S.; Day, V. W.; Jackson, T. A., *Dalton Trans.* **2011,** *40*, 1707-1715; (b) Kim, J.; Shin, B.; Kim, H.; Lee, J.; Kang, J.; Yanagisawa, S.; Ogura, T.; Masuda, H.; Ozawa, T.; Cho, J., *Inorg. Chem.* **2015,** *54*, 6176-6183; (c) Miller, C. G.; Gordon-Wylie, S. W.; Horwitz, C. P.; Strazisar, S. A.; Peraino, D. K.; Clark, G. R.; Weintraub, S. T.; Collins, T. J., *J. Am. Chem. Soc.* **1998,** *120*, 11540-11541; (d) Park, J.; Morimoto, Y.; Lee, Y.-M.; Nam, W.; Fukuzumi, S., *J. Am. Chem. Soc.* **2011,** *133*, 5236-5239.
26.As with Int1 and 8-Me, resonance Raman experiments using an Ar ion laser were attempted on aliquots of Int2 and Int3 from UV/Vis experiments. However, again ligand fluoresence precluded the observation of bands corresponding to any O-O stretches.
27.Pangborn, A. B.; Giardello, M. A.; Grubbs, R. H.; Rosen, R. K.; Timmers, F. J., *Organometallics* **1996,** *15*, 1518-1520.
28.Berliner, M. A.; Belecki, K., *J. Org. Chem.* **2005,** *70*, 9618-9621.
29.Eisch, J. J.; Piotrowski, A. M.; Han, K. I.; Kruger, C.; Tsay, Y. H., *Organometallics* **1985,** *4*, 224-231.
30.Wariishi, K.; Morishima, S.; Inagaki, Y., *Org. Process Res. Dev.* **2003,** *7*, 98-100.
31.Zhang, J. X.; Cui, Y. P.; Wang, M. L.; Liu, J. Z., *Chem. Commun.* **2002**, 2526-2527.
32.Horak, K. T.; Lin, S.; Rittle, J.; Agapie, T., *Organometallics* **2015,** *34*, 4429-4432.
33.Fulmer, G. R.; Miller, A. J. M.; Sherden, N. H.; Gottlieb, H. E.; Nudelman, A.; Stoltz, B. M.; Bercaw, J. E.; Goldberg, K. I., *Organometallics* **2010,** *29*, 2176-2179.

34.Velian, A.; Lin, S. B.; Miller, A. J. M.; Day, M. W.; Agapie, T., *J Am Chem Soc* **2010,** *132*, 6296-6297.
35.APEX2, Version 2 User Manual, M86-E01078, Bruker Analytical X-ray Systems, Madison, WI, June 2006.
36.Sheldrick, G. M. "SADABS (Version 2008/1): Program for Absorption Correction for Data from Area Detector Frames", University of Göttingen, 2008.